Thermoacclimation and genome adaptation of the membrane lipidome in marine Synechococcus

Justine Pittera, Juliette Jouhet, Solène Breton, Laurence Garczarek, Frédéric Partensky, Eric Maréchal, Ngoc Tan Nguyen, Hugo Doré, Morgane Ratin, Frances D Pitt, et al.

Thermoacclimation and genome adaptation of the membrane lipidome in marine *Synechococcus*

Justine Pittera[1], Juliette Jouhet[2], Solène Breton[1], Laurence Garczarek[1], Frédéric Partensky[1], Éric Maréchal[2], Ngoc An Nguyen[1], Hugo Doré[1], Morgane Ratin[1], Frances D. Pitt[3], David J. Scanlan[3] and Christophe Six[1]

[1] Sorbonne Universités, Université Pierre and Marie Curie (Paris 06) and Centre National de la Recherche Scientifique, UMR 7144, Marine Phototrophic Prokaryotes group, Station Biologique, Place Georges Teissier, CS 90074, 29688 Roscoff cedex, France.

[2] Laboratoire de Physiologie Cellulaire et Végétale, UMR 5168 Centre National de la Recherche Scientifique, Commissariat à l'Energie Atomique, Institut National de la Recherche Agronomique, Université Grenoble Alpes ; Institut de Biosciences et Biotechnologies de Grenoble, CEA Grenoble, 38054 Grenoble cedex 9, France.

[3] School of Life Sciences, University of Warwick, Coventry CV4 7AL, United Kingdom.

Running title: Membrane thermoadaptation in marine *Synechococcus*

Key words: temperature, membrane lipids, adaptation, phytoplankton, cyanobacteria, marine *Synechococcus*, ecotype

To whom all correspondence should be sent: Christophe Six, six@sb-roscoff.fr

Originality and significance statement

Our study constitutes the first comprehensive lipidomic work on marine *Synechococcus*, in which we show that these ecologically relevant cyanobacteria have a specific membrane lipidome structure and use particular thermoacclimation processes to maintain photosynthetic activity. Our work strongly suggests that the structure and thermoregulation of cyanobacterial membranes is thus actually much more diverse than was previously thought, to some extent rewriting the dogmas that have been established by the numerous studies on freshwater cyanobacteria. In addition, using sequences retrieved from 53 genomes, including many new genomes, we show that the enzymatic machinery catalyzing the last reactions of the membrane lipid biosynthetic pathways differ between *Synechococcus* temperature ecotypes and that a number of strains have acquired different lipid desaturation capacities through horizontal gene transfer. This work thus includes major new progress in our knowledge of the diversity and evolution of such important biosynthetic pathways. The understanding of these physiological and evolutionary processes is critical to assess how these organisms will respond to a warming planet, given their importance as key marine primary producers at the global scale.

Abstract

The marine cyanobacteria of the genus *Synechococcus* are important primary producers, displaying a wide latitudinal distribution that is underpinned by diversification into temperature ecotypes. The physiological basis underlying these ecotypes is poorly known. In many organisms, regulation of membrane fluidity is crucial for acclimating to variations in temperature. Here, we reveal the detailed composition of the membrane lipidome of the model strain *Synechococcus* sp. WH7803 and its response to temperature variation. Unlike freshwater strains, membranes are almost devoid of C18, mainly containing C14 and C16 chains with no more than two unsaturations. In response to cold, we observed a rarely observed process of acyl chain shortening that likely induces membrane thinning, along with specific desaturation activities. Both of these mechanisms likely regulate membrane fluidity, facilitating the maintenance of efficient photosynthetic activity. A comprehensive examination of 53 *Synechococcus* genomes revealed clade-specific gene sets regulating membrane lipids. In particular, the genes encoding desaturase enzymes, which are key to the temperature stress response, appeared to be temperature ecotype-specific, with some of them originating from lateral transfers. Our study suggests that regulation of membrane fluidity has been among the important adaptation processes for the colonization of different thermal niches by marine *Synechococcus*.

Introduction

Picocyanobacteria are a major component of phytoplankton communities across wide expanses of the world Ocean and responsible for up to 25% of global net marine primary production (Flombaum *et al.*, 2013). Contained within this group is the genus *Synechococcus* which occurs all the way from the equator to the poles (Zwirglmaier *et al.*, 2008; Huang *et al.*, 2012), suggesting that this widespread picocyanobacterium has developed efficient adaptive strategies to cope with temperature variations (Mackey *et al.*, 2013; Pittera *et al.*, 2014).

Marine *Synechococcus* exhibit a large genetic diversity, with 15 clades and 28 subclades delineated within the main radiation (subcluster 5.1; Herdman *et al.*, 2015) based on the *petB* gene marker encoding cytochrome b_6 (Mazard *et al.*, 2012). Phylogeography studies have shown that the major marine *Synechococcus* lineages occupy distinct ecological niches. Clades I and IV are confined to nutrient-rich, cold or temperate waters, with clade I seemingly occurring at higher latitudes than clade IV (Paulsen *et al.*, 2016), whereas clades II and III preferentially thrive in warm waters, with the former being prevalent in (sub)tropical open ocean waters and the latter dominating more oligotrophic systems, e.g. the eastern Mediterranean Sea (Sohm *et al.*, 2015; Farrant *et al.*, 2016).

Several studies have demonstrated that temperature is one of the main factors impacting the genotypic composition of marine *Synechococcus* assemblages, although other factors such as nutrients, light quantity and quality can also be important (Zwirglmaier *et al.*, 2008; Sohm *et al.*, 2015; Farrant *et al.*, 2016). Interestingly, members of *Synechococcus* clades I, II, III and IV have been shown to exhibit thermal *preferenda* consistent with the seawater temperature at their isolation site (Pittera *et al.*, 2014; Varkey *et al.*, 2016). These genetically defined lineages, physiologically adapted to specific thermal niches, therefore correspond to different temperature ecotypes, a concept previously defined for the very abundant marine cyanobacterium *Prochlorococcus* (Johnson *et al.*, 2006; Zinser *et al.*, 2007; Iskandar *et al.*, 2013).

The adaptive physiological processes conferring competitiveness to the different *Synechococcus* temperature ecotypes in their respective thermal niche remain poorly known. Membranes are among the cell components that are the most sensitive to temperature, a factor that may drastically change their fluidity and therefore the activity of membrane-embedded proteins (Mikami and Murata, 2003). Therefore, the ability to modulate membrane fluidity can be critical for the fitness of an organism in a specific thermal niche. In most freshwater and halotolerant cyanobacteria studied so far, the membrane lipid matrix comprises four main glycerolipids, including mono- and digalactosyldiacylglycerol (MGDG and DGDG, respectively), sulfoquinovosyldiacylglycerol (SQDG) and phosphatidylglycerol (PG), on which two acyl chains of usually 18 and 16 carbons long, are esterified at the *sn*-1 and *sn*-2 positions of the glycerol backbone, respectively (Fork *et al.*, 1979; Los and Mironov, 2015). Membrane fluidity can notably be adjusted by modifying the average length of

the fatty acid moiety of these glycerolipids, a thinner membrane being more fluid than a thicker one (Marsh, 2010). Another well-known mechanism, essential to tuning membrane fluidity, is the regulation of the level of unsaturation of the acyl chains, *i.e.* the number of carbon-carbon double bonds. Highly unsaturated membranes indeed exhibit increased fluidity levels and are commonly observed in cold-adapted organisms (Chintalapati *et al.*, 2007; Iskandar *et al.*, 2013).

Unsaturations are inserted into acyl chains by regiospecific enzymes called acyl desaturases. The catalytic site of these enzymes comprises histidine-rich boxes, including a non-heme iron center whose activity requires electrons and oxygen (Los and Murata, 1998; Behhrouzian and Buist, 2003). Cyanobacterial acyl desaturases have been extensively studied mostly in freshwater model organisms (Sato and Wada, 2009; Los and Mironov, 2015). For example, *Synechocystis* sp. PCC 6803 possesses four genes encoding acyl-desaturases, *desA*, *B*, *C* and *D*, which catalyze the insertion of double bonds at positions Δ12, 15, 9, and 6 of glycerolipid acyl chains (Murata and Wada, 1995). These enzymes have been shown to be major players in the temperature stress response since, by adjusting thylakoid fluidity, they notably prevent temperature-induced photoinhibition (Ludwig *et al.*, 2012; Mizusawa and Wada, 2012).

It has been reported that marine picocyanobacteria display unusual desaturase gene contents with regard to their freshwater counterparts (Chi *et al.*, 2008). A recent study by Varkey *et al.* (2016) further showed that marine *Synechococcus* strains isolated from cold waters exhibited a higher total unsaturation level than strains from warmer environments that might be related to their different sets of lipid desaturase genes. This suggests that marine *Synechococcus* use specific ways of membrane lipid regulation, which may vary depending on the thermal niches of strains. However, the lack of knowledge about the composition of membrane lipids has so far prevented a clear understanding of acclimation and adaptation mechanisms by which marine *Synechococcus* adjust their lipidomes in response to temperature changes.

Here, we analysed in detail the structure and composition of the membrane lipidome of the model marine *Synechococcus* strain WH7803 and its response to long- and short-term temperature variations. We also performed an extensive comparative genomic study of membrane lipid biosynthetic pathways in different marine *Synechococcus* ecotypes. These analyses revealed specific adaptations, notably with regard to their lipid desaturase content, which are likely critical for the ubiquity of *Synechococcus* in the marine environment.

Results

Response of Synechococcus *sp. WH7803 growth rate and photosynthesis to temperature*

Under our defined laboratory culture conditions *Synechococcus* sp. WH7803 grew between 16°C and 30°C. A plot of temperature *vs.* growth rate showed a typical shouldered shape with an abrupt drop after the optimal growth temperature was reached, which was close to 28°C (Fig. 1A). The quantum yield of the photosystem II reaction center (F_V/F_M) increased from 16°C to 25°C, reaching a maximum value of 0.65 at 25°C, before decreasing down to 0.53 at 30°C (Fig. 1B). Spectrofluorometric measurements showed that the phycoerythrin:phycocyanin fluorescence emission ratio was stable within the range 18-28°C and high at the thermal limits of growth, especially in the cold (Fig. 1C). In contrast, the fluorescence emission ratio of phycocyanin to the phycobilisome terminal acceptor remained constant at all growth temperatures. The phycourobilin:phycoerythrobilin fluorescence excitation ratio was also stable at 0.4 (data not shown). In addition, acclimation to the coldest temperature was accompanied by changes in the photosynthetic pigment ratios in the thylakoid membranes (Fig. 1D). The zeaxanthin:chl *a* mass ratio decreased from 0.52 ± 0.06 at 16°C to 0.36 ± 0.05 fg $cell^{-1}$ whilst the β-carotene:chl *a* mass ratio remained stable at 0.12 ± 0.10. These variations in pigment ratios suggest a decrease of the chl *a* and β-carotene cell content relative to zeaxanthin (Kana *et al.*, 1988; Moore *et al.* 1995; Six *et al.* 2004).

Composition of the membrane lipidome in Synechococcus *sp. WH7803*

Separation of membrane lipid classes by 2-dimensional thin layer chromatography showed four major spots that corresponded to the four lipid classes typical of cyanobacteria, MGDG, DGDG, SQDG and PG (Fig. S1). We did not detect the galactolipid precursor monoglucosyldiacylglycerol (MGlcDG) with the lipid quantities we loaded on the plates. LC-MS/MS analyses showed that the proportions of each glycerolipid remained stable at all growth temperatures, with MGDG being the dominant lipid (45.4 ± 4.1 %) followed by DGDG (23.0 ± 3.6 %) and SQDG (24.1 ± 3.9 %). PG was a minor lipid in these membranes (7.5 ± 2.3 %). In contrast to most freshwater strains, the fatty acid moiety of *Synechococcus* sp. WH7803 lipids mostly comprised C14 and C16 chains, with only traces of C18 chains (Meritt *et al.*, 1991) and no more than two unsaturations per chain were detected. Although our analyses do not provide this information, it is likely that the unsaturated fatty acid species were $C14{:}1^{\Delta 9}$, $C16{:}1^{\Delta 9}$, $C18{:}1^{\Delta 9}$ and $C16{:}2^{\Delta 9,12}$, as in all other cyanobacteria described so far (Los and Mironov, 2015). The *sn*-1 position most often bind a C16 chain, whereas C14 chains were more frequent at the *sn*-2 position.

Molecular thermoacclimation of the glycerolipids in Synechococcus *sp. WH7803*

The global membrane lipidome showed clear responses to long- and short-term temperature variations. Whereas the proportion of the four glycerolipids did not vary, the fatty acid moieties of the

three glycolipids were modified in response to temperature. With decreasing growth temperature, the average acyl chain length of the galactolipids decreased and the global proportion of unsaturated chains in the membranes strongly increased from 33.4 ± 0.9 at 30°C to 54.5 ± 0.4 % at 16 °C (Table S1). We hereafter present the molecular changes specific to each glycerolipid, which explain these observed global changes.

Monogalactosyldiacylglycerol – The acyl chain esterified at the *sn*-2 position of MGDG was invariably a C14 chain, whereas the *sn*-1 position was most often a C16 chain (Fig. 2, Tables S2, S3). The average length of the MGDG *sn*-1 acyl chain slightly decreased with decreasing temperature, from about 15.8 carbon atoms at 28-30°C to 15.3 carbon atoms at 16°C (Table S3), due to an increase in the monounsaturated C14:1 at the expense of the C16 chains. This C14:1 synthesis did not seemingly originate in a dynamically induced desaturation of C14:0 chains, since the latter chains were not abundant and did not decrease proportionally (Fig. 2, Table S2). C14:1 synthesis was not observed when cells acclimated to 22°C were suddenly shifted to 18°C and 13°C for 4 days (Fig. 3A, B). However, when cells were shifted to 30°C, the reverse reactions were completed after 24 h (Fig. 4A, B).

Only two weak desaturation activities were detected on the MGDG. At the *sn*-2 position, some C14:0 chains were desaturated into C14:1, the latter being undetectable at temperatures higher than 25°C (Fig.2, Table S2). Similarly, a small fraction of the C16:1 chains at the *sn*-1 position were desaturated into C16:2 (Fig. 2, Table S2). These two reactions were also apparent during the cold-shift experiments. When cells acclimated to 22°C were shifted to 13°C, the *sn*-1 C16:2 was synthesized up to 10% of the MGDG *sn*-1 bound chains, while the *sn*-1 16:1 chain decreased from a similar proportion (Fig. 3B). This desaturation was hardly detectable when cells were shifted to 18°C, with less than 0.5% 16:2 at the end of the experiment. Both cold shifts induced the synthesis of C14:1 at the *sn*-2 position, but this was stronger at 13°C (Fig. 3C).

Digalactosyldiacylglycerol – The acyl chains esterified to DGDG were similar to those of the MGDG, as the glycerol *sn*-2 position was exclusively occupied by a C14 chain, almost systematically saturated, whereas the *sn*-1 position was dominated by C16 chains (Fig. 2, Tables S2, S3). As for MGDG, a shortening of the *sn*-1 position by synthesis of C14:1 was observable. This was also induced during the cold-shift experiments (Fig. 3E) and the reverse reactions were completed one day after cells were shifted from 22°C to 30°C (Fig. 4E).

Similar to MGDG, we observed at the lowest acclimation temperatures a slight induction of C14:1 at both *sn*-2 and *sn*-1 positions and C16:2 at the *sn*-1 position (Fig. 2, Table S2). These weak desaturation activities were also detected during the two cold-shift experiments (Fig. 3E, F). In contrast to MGDG, the C16:0 chain of the DGDG sn-1 position was the site of a strong desaturation activity. Cells acclimated to 30°C showed 75% C16:0 and 11 % C16:1 at this position whereas at 16°C, C16:0

decreased to 18% while C16:1 increased to 51% (Fig. 2). This monodesaturation was also strongly induced in both cold shift experiments and the reverse reaction was rapidly induced when cultures were shifted from 22°C to 30°C (Fig. 3D, 4D, E).

Sulfoquinovosyldiacylglycerol – In contrast to the galactolipids, SQDG *sn*-2 acyl chains included both C14 and C16 chains, with roughly 50% of each. However, at 16°C there was more C14, indicating a shortening of the average chain length at this position (Fig. 2, Tables S2, S3). Comparable variations were observed during the temperature shift experiments. The acyl chains bound at the *sn*-1 position were predominantly C16 chains (with only 4-7% C14), independent of the growth temperature (Fig. 2, Table S2).

With decreasing growth temperature, the *sn*-2 position was enriched in C16:2 whereas the *sn*-1 position bound more C14:1 and much more C16:1, as the result of the desaturation of the C14:0 and C16:0 chains (Fig. 2, Table S2). Similar variations were observed during both cold shift experiments, with desaturation activities more marked when the cells were shifted from 22°C to 13°C (Fig. 3G, H). The reverse reaction 16:1 -> 16:0 was induced at high efficiency when cells were shifted from 22°C to 30°C (Fig. 4G, H).

Phosphatidylglycerol – PG appeared to be totally different from the three glycolipids as no C14 was detected and the PG molecules contained almost only C16 chains. Some C18:1 chains were occasionally detected at the *sn*-1 position (Fig. 2, Table S2). Overall, the composition in acyl chains was dominated by C16:1 chains, and poorly influenced by temperature (Fig. 2, 3J, K, L, and Table S2). Some slight variations were however observed during shifts from 22°C to 30°C, mostly comprising a decrease in the 16:1:16:0 ratio at the *sn*-2 position (Fig. 4J, K, L).

Membrane lipid biosynthetic pathways in marine Synechococcus *and* Cyanobium

The bacterial fatty acid synthase (FAS II) has been extensively studied in *Synechocystis* sp. PCC 6803 (see *e.g.* Liu *et al*., 2011; Hu *et al*., 2013). However, the dearth of knowledge of these enzymes in marine *Synechococcus* spurred us to search the 53 complete *Synechococcus* and *Cyanobium* genomes for homologs of known FAS II genes. Expectedly, most of the genes involved in the FAS II pathway are present as a unique copy in all the searched genomes, including the four enzymes (AccA-D) comprising the initiation module and the following steps catalyzed by the β-ketoacyl-ACP synthase III (KAS III), the β-ketoacyl reductase (KR), the β-hydroxyacyl-ACP dehydratase (DH) and the enoyl-ACP reductase (ENR). In cyanobacteria, the KAS II enzyme is thought to be responsible for the entire fatty acid elongation, condensing the growing acyl-ACP with malonyl-ACP to extend the chain by adding two carbons at each cycle (White *et al.*, 2005). Search for KAS II in *Synechococcus* genomes revealed that all of them possess at least one *fabF* gene copy but, interestingly, 20 out of 53 strains, mostly belonging to clades II, III, IV and WPC1, actually possess a second copy that we called *fabF2* (Table S4). Both

copies are significantly more related to *E. coli fabF* (KAS II; e.g. 54 and 38 % aa identity of WH8102 FabF and FabF2 to *E. coli* K12 FabF, respectively) than they are to *fabB* (KAS I; 38 and 29 % aa identity of WH8102 FabF and FabF2 to *E. coli* K12 FabB, respectively).

The incorporation into the membranes starts with the acylation of G3P catalyzed by the PlsX-GPAT system, then the membrane-associated protein PlsX catalyzes the formation of an acyl-phosphate (Acyl-P; Cross, 2016) and the G3P acyltransferase (GPAT) acylates the 1-position of G3P forming lysophosphatidic acid (LPA). Finally, the LPA acyltransferase (LPAAT) acylates the *sn*-2 position of LPA to form phosphatidic acid (PA), the central intermediate of membrane glycerolipids. All these enzymes are encoded by single core genes in the *Synechococcus* and *Cyanobium* genomes.

The biosynthetic pathways of membrane lipids in cyanobacteria then divide into two branches, leading to the synthesis of the glycolipids or to PG (Petroutsos *et al.*, 2014). For the galactolipid pathway, an ortholog of the PA phosphatase (Nakamura *et al.*, 2007) is present in four halotolerant strains (CB0101, CB0205, WH5701 and PCC 6307) but not in the 'truly' marine *Synechococcus* strains, suggesting that another enzyme is involved in this process in the latter strains. A possible candidate is a membrane protein possessing a PA phosphatase-like domain (Cyanorak cluster CK_0000099). The diacylglycerol produced is then used as a substrate for the synthesis of MGlcDG, which in cyanobacteria, is further epimerized into MGDG (Awai, 2016). In many freshwater cyanobacterial strains, the MGlcDG epimerase is encoded by the *mgdE* gene (Awai *et al.*, 2014; Sato, 2015), which includes a C-terminus Rossmann fold domain and a fatty acid hydroxylase at the N-terminus, the function of which remains unclear (Awai, 2016). In marine *Synechococcus*, the best hit to *mgdE* is a gene that includes only the C-terminal Rossmann-fold domain of the *Synechocystis* gene (Table S5). DGDG is synthesized from MGDG by the *dgdA* gene product (Sakurai *et al.* 2007), and SQDG by the UDP-sulfoquinovose synthase (SqdB) and the SQDG synthase (SqdX; Sanda *et al.*, 2001). PG is synthesized by the phosphatidyl-glycerophosphate synthase (PgsA). All these proteins are encoded by single core genes in marine *Synechococcus* spp. (Table S5). Additional information is available in the supplementary material.

<u>*Lipid desaturases in marine* Synechococcus and Cyanobium</u>

The acyl desaturases of marine cyanobacteria have so far been poorly studied, even though they have already been reported to differ from those of their freshwater counterparts (Chi *et al.*, 2008; Varkey et *al.*, 2016). We identified 11 gene clusters encoding putative lipid desaturase enzymes (Table 1), with one to six desaturases per strain. These genes encode proteins ranging from 259 to 428 amino acids, as compared to 318 to 359 amino acids in *Synechocystis* sp. PCC 6803 (Murata and Wada, 1995).

Phylogenetic analysis of the 11 marine acyl desaturases together with freshwater cyanobacteria desaturases (Fig. 5, datasets 1-2) and comparison of their 3 conserved histidine-rich

motifs with those previously determined based on 37 cyanobacterial genomes (Chi *et al.*, 2008; Fig. S2-4), allowed us to identify six major marine *Synechococcus* lipid desaturases, including three putative Δ9 desaturases (DesC3, C4, C6; Fig. S2) and three putative Δ12 desaturases (DesA2, A3, A4; Fig. S3). In addition, five other proteins, present only in one or two *Synechococcus* strains (Table 1), also displayed two to three histidine-rich motifs but could not be assigned with confidence to a specific desaturase type (Fig. S4). Each of the six major desaturases indeed form well-supported monophyletic groups within the DesC or DesA/B clusters, and their histidine-rich motifs were typical of Δ9 or Δ12 desaturases, respectively (more details in the supplemental material). Noteworthy, while DesC3 and DesC4 display a quite high degree of similarity between strains, and especially within sub-cluster 5.1 (Average % identity: 87.3 % and 85.5 %, respectively), DesA2 and particularly DesA3 sequences proved to be much more variable with 79.4 % and 58.5% identity on average within sub-cluster 5.1, respectively.

In order to decipher the origin and evolution of this gene family in marine *Synechococcus*, the phyletic profiles (Table 1), the genomic context of each gene (Fig. 6), their potential occurrence in genomic islands (Fig. 6), the local nucleotide composition (Fig. S7) and their phylogenetic relatedness (Fig. S5-6 and S8-9) were examined for the 4 main acyl-desaturases. While *des*C3 is a core gene, *i.e.* present in all strains, the *des*C4 gene is specifically absent from clades II, III, WPC1, XX and UC-A (Table 1). Although there is little doubt given their close phylogenetic relatedness that the accessory *des*C4 gene arose from a duplication event of the core *des*C3 gene ancestor (Fig. 5), it is difficult to conclude with certainty whether the absence of *des*C4 in clades II, III, WPC1, XX and UC-A is due to a specific loss in these lineages after their diversification, or to a loss (in their common ancestor with clade IV), followed by a secondary reacquisition of this gene in clade IV strains by lateral transfer, potentially from clade I (Fig. S6; more details in the supplementary material).

As for the *des*A2 gene, although the genomic context is very well conserved among most strains of sub-cluster 5.1, it is very different in strain BIOS-U3-1 (clade CRD1), and in both sub-cluster 5.2 strains CB0101 and CB0205, suggesting that this gene has been laterally transferred in these lineages (Fig. 6). This is supported for BIOS-U3-1 both by Alien Hunter genomic island prediction (Fig. 6) and comparative phylogenetic analyses (Fig. S8), and for CB0101 and CB0205 by the absence of *des*A2 in all other 5.2 strains (Table 1). As concerns *desA3*, both its highly variable genomic context between strains (data not shown) and comparative phylogenetic analyses (Fig. S9), which group together strains distantly related based on ribosomal protein phylogeny (belonging to clades II, IV, XX and 2 out of the 3 clades VII strains), strongly suggest the occurrence of multiple lateral transfers for this gene. This hypothesis is further strengthened by the detection of this gene in a genomic island for 12 out of 53 *Synechococcus* strains (Fig. 6).

Discussion

Growth and photosynthesis response to temperature

Synechococcus sp. WH7803 that was isolated in the Sargasso Sea in summer, *i.e.* in rather warm waters (25.8°C; Pittera *et al.*, 2014), displays a thermal *preferendum* corresponding to warm temperate ecotypes. In this study, under continuous low light irradiance (20 µmol photons m^{-2} s^{-1}), we were able to grow this strain from 16°C to 30°C, with an optimal growth rate at ca. 28°C. Curiously, growing this strain under the same conditions, but at a light intensity of 80 µmol photons m^{-2} s^{-1}, extended the thermal growth range up to 34°C with optimal growth at 33°C (Pittera *et al.*, 2014). This shows that *Synechococcus* growth capacity depends on the interaction between light and temperature, as seen for other cyanobacteria (Miśkiewicz *et al.*, 2000) and phytoplankton (Edwards *et al.* 2016), the latter study showing that light-limitation can reduce the optimal growth temperature of phytoplankton by ~5°C.

Synechococcus sp. WH7803 cells were able to maintain high photosynthetic efficiency throughout the thermal growth range as shown by the photosystem II quantum yield which was generally higher than 0.5. The maximal yield was close to 25°C, *i.e.* at a temperature slightly lower than the maximal growth temperature, indicating that optimal photosynthesis is not necessarily coupled to optimal growth over a temperature range. Photosystem II quantum yield was lower at the thermal growth limits, especially at 16°C, probably due to chronic photoinhibition and/or non photochemical quenching of fluorescence. It is worth noting that the phycoerythrin fluorescence increase at 16°C (see below) also contributes to the low F_V/F_M at this temperature since, in cyanobacteria, phycobiliprotein fluorescence contributes much to the F_0 fluorescence level (Ogawa *et al.*, 2017).

The functioning of the photosynthetic antenna, the phycobilisome, was also disturbed at the thermal growth limits. Indeed, *in vivo* fluorescence emission spectra showed an increase of phycoerythrin fluorescence relative to phycocyanin, indicating a chronic decrease of the energy transfer rate, *i.e.* an energy leak, between these two phycobiliproteins. This impairment, mostly visible at 16°C, is likely related to a temperature induced change of conformation of the phycobiliproteins. Indeed, Pittera *et al.* (2016) recently showed that the stability of marine *Synechococcus* phycobilisomes varies according to the average sea surface temperature at the strain isolation site. The phycoerythrin fluorescence increase can also be interpreted as a way to dissipate excess light at a temperature at which it cannot be fully utilized by the photosystem reaction centers. In addition, our pigment analyses show a response to temperature that mimics high light acclimation (Kana *et al.*, 1988; Moore *et al.*, 1995; Six *et al.* 2004). This has been described in numerous photosynthetic organisms and notably implies the down regulation of the photosystem cell content, in order to adjust light utilization capacities at low temperature. In *Synechococcus* sp. WH7803, these processes are observable only at

the cold growth limits, suggesting that other mechanisms stabilize the photosynthetic apparatus throughout the rest of the thermal growth range.

Cold-induced changes in membrane composition and thickness

Thylakoid membranes are by far the predominant membranes in cyanobacteria and thus their lipid composition is close to that of the total cellular membranes (Sakurai *et al.*, 2006). Membrane fluidity adjustments are critical for the biological reactions occurring in membranes, particularly in thylakoids. Membrane fluidity is in large part determined by the ambient temperature, the degree of unsaturation and the length of the constituent fatty acids (*i.e*. membrane thickness). We did not observe any significant changes in the proportions of the four main membrane lipids, indicating that *Synechococcus* sp. WH7803 does not acclimate to temperature variations by modifying the polar lipid head groups in the membranes. MGDG was always the dominant lipid, followed by DGDG, SQDG and PG, as commonly described in freshwater cyanobacteria and eukaryotic chloroplasts (see *e.g.* Murata *et al.*, 1992; Somerville *et al.*, 2000; Wada and Mizusawa 2009; Dormann and Holzl, 2009; Shimojima *et al.*, 2009a; Awai, 2016). Our data are thus somewhat at odds with studies by Van Mooy *et al.* (2006, 2009) that describe marine *Synechococcus*, *Prochlorococcus* and the model freshwater cyanobacterium *Synechocystis* sp. PCC 6803 as containing relatively less MGDG, a surprising result in view of the numerous reports of the membrane composition of the latter, intensively studied strain (Awai *et al.*, 2014; Sato and Wada, 2009). Indeed, a recent study reported MGDG as the dominant membrane lipid in several strains of the marine picocyanobacterium *Prochlorococcus* (Biller *et al.*, 2014).

In many freshwater cyanobacteria, MGlcDG, the precursor of MGDG, is often detected in lipidomic analyses. In *Synechocystis* sp. PCC 6803, the MGlcDG synthase MgdA is activated by high temperature whereas MgdE is inhibited, leading to the accumulation of MGlcDG (Shimojima *et al.*, 2009b; Awai *et al.*, 2014). In marine *Synechococcus*, the best hit to *mgdE*, encoding the MGlcDG epimerase, is a gene that includes only the C-terminal Rossmann-fold domain of the *Synechocystis* gene (Table S5), suggesting that the fatty acid hydroxylase domain is probably not essential to the epimerase activity. However, we did not notice such MGlcDG accumulation in high temperature acclimated cells nor in warm shift experiments.

Synechococcus sp. WH7803 membranes seem to contain only traces of C18 chains and are C14-rich, whereas most freshwater strains bind C18 fatty acids at the *sn*-1 position of the glycerol backbone on all lipids, and a shorter C16 chain at the *sn*-2 position (Sato and Wada, 2009; Los and Mironov, 2015). The glycolipids of *Synechococcus* sp. WH7803 have nevertheless a similar global structure to the freshwater strain lipids, as the glycerol *sn*-1 position most often binds a C16 chain, and the *sn*-2 position a shorter C14 chain. Consequently, *Synechococcus* sp. WH7803 membranes are on average thinner

than most freshwater strains. This feature might be related to the constraint of the picoplanktonic size of this type of organism and/or an adaptation trait to high salt environment, as membrane fluidization is a response mechanism to salt stress in many microorganisms (Los and Murata, 2004; Rodriguez-Vargas *et al.*, 2007). The nature of the fatty acid bound to the *sn*-2 position is regulated by the acyl-ACP pools and the lysophosphatidic acid acyltransferases (*plcC*), which may have different affinities for specific fatty acid lengths. The two distinct enzymes present in the genome of *Synechococcus* sp. WH7803, like in all other marine *Synechococcus* (Table S5), may be responsible for this possibility to bind either a C14 or a C16 chain at the *sn*-2 position, as shown in *Synechocystis* sp. PCC 6803 for C16 and C18 chains (Okazaki *et al.*, 2006).

Our results suggest that variations in the acyl chain length are involved in the response to temperature in *Synechococcus* sp. WH7803. At the *sn*-1 position of both galactolipids, a significant proportion of the C16 chains were replaced by C14:1 in response to cold. Since there was no apparent concomitant desaturation of the myristic acid chains (C14:0), it is likely that C14:1 were synthesized *de novo* to replace C16 chains. This induced both a shortening and an increase of the unsaturation level of the galactolipids at the glycerol *sn*-1 position, likely leading to an increase in membrane fluidity in response to cold temperature. The *de novo* synthesis is also supported by the fact that this mechanism was observed only in long-term thermoacclimated cells and warm shift experiments, as *de novo* synthesis requires time and metabolically active cells. SQDG was not subjected to such a process.

Determination of the length of the acyl chains is thought to rely on a complex enzymatic regulation system, based on competition among elongation synthases, the supply of malonyl-ACP and the utilization of acyl-ACPs by the acyltransferase (Heath *et al.*, 1994; Heath and Rock, 1995). It has also been shown that the β-ketoacyl synthase II is essential for the regulation of fatty acid composition in response to temperature fluctuations (Garwin *et al.*, 1980, Heath *et al.*, 2002). The regulatory role of KAS enzymes in the length of fatty acid chain synthesis has notably been evidenced by the characterization of KAS IV enzymes, which display strong preferences for the elongation of short chain acyl-ACPs (Schutt *et al.*, 2002). Interestingly, searches for KAS II in the *Synechococcus* and *Cyanobium* genomes revealed they all possess at least one *fabF* gene copy, but 20 out of 53 strains, mostly belonging to clades II, III, IV and WPC1, actually possess an additional gene copy, *fabF2* (Table S4). The function of this second KAS II remains unclear but one might hypothesize that it is related to a ecotype-specific ability to incorporate different lengths of acyl chains into the membranes, in order to modulate the fluidity in response to temperature changes.

Cold-induced desaturations of acyl chains in Synechococcus sp. WH7803

The extent of unsaturation of the fatty acids in *Synechococcus* sp. WH7803 is rather low, as only mono- and dienoic acyl chains were detected. The fatty acid desaturation activities were more

pronounced when the cells were transferred to 13°C than at 18°C, clearly showing the temperature sensitivity of the acclimation system. The results of the warm shift experiment (30°C) also support this and illustrate well the dynamic plasticity of the membrane lipidome of *Synechococcus* sp. WH7803.

At the *sn*-2 position of both galactolipids, a weak cold-induced desaturation activity induced the conversion of C14 chains into C14:1 chains, as seen in the fully acclimated cells and the cold shift experiments. Similarly, low amounts of C16:2 were synthesized in response to cold only in the galactolipids. The major cold-induced desaturation activities occurred on the C16 chains at the *sn*-1 position of the SQDG and the DGDG, leading to efficient conversion of palmitic acid into palmitoleic acyl chain. These two reactions were immediately induced upon a rapid temperature decrease, reaching a plateau corresponding to the long-term acclimated state in about 24 h (Fig. 3D, E, G, H). SQDG was the only lipid that could be desaturated at the *sn*-2 position (C16:0 -> C16:1) in response to cold temperature, although to a low extent.

When all these processes are summed, the total cell content of unsaturated acyl chains significantly increases from about 35% at 30°C to 55% at 16°C. These are values comparable to the study of Varkey *et al.* (2016), who measured the percentage of unsaturated fatty acids in three *Synechococcus* strains acclimated to two different temperatures. These mechanisms differ from those known in freshwater cyanobacteria since so far there has been no positive evidence for a desaturation activity on DGDG in the latter organisms (Sato and Wada, 2009). However, studies on *Synechocystis* mutants devoid of DGDG showed that this galactolipid is involved in thermotolerance by influencing the sensitivity to photoinhibition at different temperatures (Mizusawa *et al.*, 2009a, 2009b). By contrast, in the marine *Synechococcus* sp. WH7803, we show here that DGDG is a major target for cold-induced acyl desaturation.

In *Synechococcus* sp. WH7803, PG is a minor lipid that appears quite different from the three main glycolipids. At both glycerol positions, the dominant acyl chain was palmitoleic acid whilst C18:1 chains were occasionally detected at the *sn*-1 position. In contrast to most freshwater strains in which the C18 chain bound to the *sn*-1 position can be desaturated (Sato and Wada, 2009), the fatty acid content of PG did not show any clear desaturation response to temperature acclimation. In *Synechocystis* sp. PCC 6803 and *Synechococcus* sp. PCC 7942, a number of mutant studies have demonstrated that PG is physiologically essential and is notably involved in the activity of both photosystems, influencing the dimerization and reactivation of core complexes (Sakurai *et al.*, 2003; Yamamoto, 2016; Bogos *et al.*, 2010). X-ray crystallographic analysis of photosystem II at 1.9 Å resolution has identified 5 PG molecules bound to photosystem II, directly connected to the D1 protein and plastoquinone Q_B (Itoh *et al.*, 2012; Mizusawa and Wada, 2012). It is thus probable that low amounts of PG in *Synechococcus* sp. WH7803 are associated with PSII, playing an important structural role that requires a fixed composition in fatty acids.

Evolution of the desaturase family in marine Synechococcus

The desaturation of fatty acids involves O_2-dependent dehydrogenation reactions catalyzed by non-heme di-iron desaturase enzymes *via* an electron donor molecule (Los and Murata, 1998; Behhrouzian and Buist, 2003). These reactions are highly stereoselective and regioselective, a desaturase being able to insert a double bond at a specific position of the fatty acid, located at a given *sn*- position on the glycerol backbone. These enzymes, which prevent membranes from undergoing transition to the gel phase, a state which is lethal for cells, are encoded by cold-inducible genes that have been well characterized in *Synechocystis* sp. PCC 6803 (see *e.g.* Sato and Wada, 2009). We screened 53 genomes of marine and halotolerant *Synechococcus*/*Cyanobium* for lipid desaturase genes. Whereas freshwater (Los and Mironov, 2015) and halotolerant (this study) strains often contain a high number of desaturase genes, most of the truly marine *Synechococcus*, belonging to subcluster 5.1, usually contain three or four genes encoding DesC3, DesC4, DesA3 and DesA4 proteins. This number is even lower for clade II, for which most of the representative strains have only two desaturase genes. This suggests that these warm-adapted cyanobacteria have a globally low capacity to modulate membrane fluidity, consistent with their thermal niche. The variability in lipid-desaturase gene number among *Synechococcus* strains can also be seen as an adaptation to low seasonal variability in warm, tropical waters compared to strong seasonality at higher latitudes. More generally, the globally low number of desaturase genes in marine *Synechococcus* is in agreement with the low level of unsaturation that we observed in the model strain WH7803, which contains four desaturase genes, and therefore expected to be able to undertake only two types of Δ9-desaturations and two types of Δ12-desaturations.

In freshwater cyanobacteria that contain both *desC1* and *desC2* genes, the products of these genes insert an unsaturation at the ninth carbon from the carboxyl end of the C18 acyl chain bound at the *sn*-1 position and the C16 chain bound at the *sn*-2 position, respectively. Although this requires experimental evidence, it is thus possible that the marine DesC3 and DesC4 enzymes carry out the Δ9-desaturation activities on the palmitic (C16:0) and myristic (C14:0) chains which, similar to freshwater strains, are most often bound to the *sn*-1 and *sn*-2 glycerol positions of the membrane lipids in *Synechococcus* sp. WH7803, respectively.

The phylogenetic relatedness of *desC3* and *desC4* as well as their immediate vicinity in genomes suggests that these genes originate from a duplication event. In freshwater cyanobacteria, DesC1 is usually a constitutive enzyme whose activity is not necessarily temperature induced, while DesC2 desaturates the acyl chain at the *sn*-2 position in response to cold stress (Chintalapati *et al.*, 2006, 2007). By analogy, DesC3, a Δ9 desaturase present in all marine *Synechococcus* genomes, could be a constitutive enzyme that likely desaturates the acyl chains bound to the *sn*-1 position. As for

DesC4, among the phylogenetic clades whose thermal niche has been studied (Pittera *et al.*, 2014; Farrant *et al.*, 2016), it is only absent in clades adapted to warm environments (clades II and III). Thus, similarly to DesC2 in freshwater cyanobacteria, DesC4 could well provide additional Δ9 desaturation capacity, which would be induced under cold conditions (Varkey et *al.* 2016). The fact that DesC4 is present in most *Synechococcus* strains (except clades II and III), including halotolerant members of sub-cluster 5.2, tends to support the hypothesis that this gene has been lost in the warm-adapted clades II and III, rather than gained in all other clades.

The two marine enzymes DesA3 and DesA4 are expected to be responsible for the few double unsaturations (C16:2) that we detected in *Synechococcus* sp. WH7803, located exclusively on the *sn*-1 of the two galactolipids. These double unsaturations appear to be scarce and only induced when the cells were acclimated to a temperature lower than the optimal growth temperature. In this context, the specificities of the two enzymes DesA3 and DesA4 in *Synechococcus* sp. WH7803 remain unclear, but one may hypothesize that each of them acts on a specific galactolipid. DesA3 is present in almost all marine *Synechococcus* and *Cyanobium*, but is absent from most strains of the tropical clade II. Interestingly, the only clade II strains possessing DesA3, PROS-U-1 and WH8109, were isolated from an upwelling area located off the Moroccan coast and in northern water of the Sargasso Sea, where the temperature is rather low compared to tropical waters (Pittera *et al*., 2014). Thus, in addition to the absence of the DesC4 enzyme, clade II ecotypes, adapted to the warmest waters of the world Ocean, also exhibit decreased capacities to synthesize dienoic acyl chains, compared to most marine *Synechococcus*. Although the phyletic profile of *des*A2 is a bit less clear cut, it seems that DesA2 is counter selected in cold environments (clades I and IV habitats) and mostly found in strains isolated in rather warm waters (clades II, III, V and VI; Pittera *et al.*, 2014). Still, characterization of its function is necessary to better understand its potential significance for thermal niche adaptation.

Conclusion

Several studies suggest that thylakoids require a particularly high level of fluidity regulation for the proper functioning of the embedded proteins, which occupy about 70% of the membranes (Kirchhoff *et al*., 2008; Dormann and Holzl, 2009; Yamamoto, 2016). As these membranes provide the matrix for the photosynthetic machinery, the fluidity regulation processes we highlight in this study are likely essential mechanisms for survival and competitiveness of a cyanobacterial strain at different temperatures. Our results show that the marine picocyanobacterium *Synechococcus* sp. WH7803 maintains optimal photosynthetic rates over most of its growth temperature range. To do so, this cyanobacterium undergoes a remodeling of the composition of the acyl moiety of the membrane lipids in order to adjust membrane fluidity. The membrane lipidome regulation mechanisms used by this

marine strain notably rely on specific desaturation processes of *sn*-1 bound acyl chains of the three glycolipids, as well as a shortening of the *sn*-1 position of the major membrane constituents, the galactolipids. The latter temperature-induced process has so far only been rarely reported (Shivaji and Prakash, 2010). In organisms that use a limited set of desaturase enzymes, such a mechanism may constitute an important additional component of the response to thermal changes in order to adequately adjust membrane fluidity and successfully acclimate to temperature variations. These processes constitute significant differences with the mechanisms described so far in freshwater cyanobacteria.

Our study shows that, during the diversification of the marine *Synechococcus* radiation into different temperature ecotypes, membrane lipid metabolism pathways have been globally well conserved. However, the enzymatic machinery catalyzing the last reactions of the biosynthetic pathways seem to be less evolutionary constrained and distinct *Synechococcus* ecotypes have acquired different lipid desaturation capacities, notably through horizontal gene transfer events. These mechanisms appear to be directly linked to temperature adaptation and niche partitioning, since *Synechococcus* ecotypes adapted to the warmest environments generally show lower fatty acid desaturation capacities than those adapted to temperate and subpolar waters. This observation highlights the importance of the capacity of *Synechococcus* cells to regulate their membrane composition for colonizing distinct thermal niches, likely a key factor for the ecological success of these picocyanobacteria in the world Ocean. Future studies should aim at characterizing the biochemical function of thermotype-specific lyases, e.g. through gene inactivation and heterologous expression approaches.

Experimental procedures

Culture conditions and experimental design

The axenic strain *Synechococcus* sp. WH7803 was retrieved from the Roscoff culture collection (http://roscoff-culture-collection.org/) and grown in PCR-S11 culture medium (Rippka *et al.*, 2000) supplemented with 1 mM sodium nitrate. Continuous light was provided by multicolor LED systems (Alpheus, France) at 20 µmol photons m^{-2} s^{-1} irradiance. The axenic nature of the cultures was regularly checked by flow cytometry using SYBR-Green staining.

To study the temperature induced differences in the homeostatic composition of the membranes, cultures were acclimated for several weeks to a range of temperatures, from 16 to 30°C, within temperature-controlled chambers, and sampled during the exponential growth phase. To study the dynamics of the temperature-induced remodeling of the membranes, we carried out temperature shift experiments. Ten liters of early exponentially growing cultures maintained at 22°C were split and

transferred to 13, 18 or 30°C, under identical light conditions. Then, the subcultures were sampled during four days. All experiments were repeated at least three times.

Flow Cytometry, in vivo *fluorometry and pigment analyses*

Aliquots of cultures were preserved using 0.25% (v/v) glutaraldehyde (grade II, Sigma Aldrich, St Louis, MO, USA) and stored at -80°C until analysis. Cell concentrations were determined using a flow cytometer (FACS Canto II, Becton Dickinson, San Jose, CA, USA), as described previously (Marie *et al.*, 1999). Growth rates were computed as the slope of a Ln(Nt) *vs*. time plot, where Nt is the cell concentration at time t.

The photosystem II quantum yield (F_V/F_M) was measured using a Pulse Amplitude Modulation fluorometer (PhytoPAM, Walz, Effeltrich, Germany) in the presence of 100 mM of the PSII blocker 3-(3,4-dichlorophenyl)-1,1-dimethylurea, following a previously described procedure (Pittera *et al.*, 2014). The quantum yield was calculated as:

$$F_V/F_M = (F_M - F_0)/F_M$$

where F_0 is the basal fluorescence level, F_M the maximal fluorescence level and F_V is the variable fluorescence (Campbell *et al.*, 1998; Ogawa *et al.*, 2017).

Furthermore, in order to study phycobiliprotein coupling in the phycobilisome, fluorescence emission spectra were recorded with a LS-50B spectrofluorometer (Perkin-Elmer, Waltham, MA, USA), as described elsewhere (Pittera *et al.*, 2016). Fluorescence excitation spectra were recorded to determine the phycourobilin to phycoerythrobilin ratio (Six *et al.*, 2007).

For pigment analyses, 50 mL volumes of culture were harvested by centrifugation in the presence of 0.01% (v/v) pluronic acid final concentration (Sigma Aldrich, St Louis, MO, USA). After extraction in methanol, pigment extracts were supplemented with distilled water. Pigments were then measured by high pressure liquid chromatography using an HPLC 1100 Series System (Hewlett Packard, St Palo Alto, CA, USA), as described previously (Pittera *et al.*, 2014).

Membrane lipidome analyses

Lipid extraction - Cells were harvested by centrifugation and stored at -80°C until analysis. Membrane lipids were extracted in glass hardware following a modified version of the Bligh and Dyer (1959) procedure, using methanol/dichloromethane/water at ratios of 1.1/1/1.4, then evaporated under nitrogen and stored at -20°C until analysis.

Fatty acid regiolocalization - We first identified the positional distribution of the fatty acids esterified to the four main glycerolipids of *Synechococcus* sp. WH7803. To do so, 400 mL culture grown at 16, 22 and 30°C was harvested and the lipids extracted as described above. The glyceroplipid classes were separated by 2-dimensional thin layer chromatography on 20 x 20 cm silica plates (Merck, Darmstadt,

Germany), using chloroform/methanol/water and chloroform/acetone/methanol/acetic acid/water at ratios of 65/25/4 and 50/20/10/10/5 v/v, respectively, (Simionato *et al.*, 2013). Glycerolipid spots were revealed under UV light in the presence of 8-anilino-1-naphthalene sulfonic acid (0.2 % in pure methanol) and scraped off the plates. Each separated lipid class was recovered from the silica powder after addition of 1.35 mL chloroform:methanol 1:2 v/v, thorough mixing and addition of 0.45 mL chloroform and 0.8 mL H_2O and collection of the chloroform phase. Lipids were then dried under argon and analyzed by mass spectrometry (MS). Purified lipid classes were dissolved in 10 mM ammonium acetate in pure methanol. The glycerolipids were introduced by direct infusion (ESI-MS) into a trap type mass spectrometer (LTQ-XL, Thermo Scientific), and their identity was confirmed by MS/MS analysis as described in Abida et al. (2016). Under these conditions, the produced ions were mainly present as H^-, H^+, $NH4^+$ or Na^+ adducts. The position of the fatty acid molecular species esterified to the glycerol backbone of the purified glycerolipids was determined by MS/MS analyses. Depending on the glycerolipid species and the ionic adduct, the substituents at *sn*-1 and *sn*-2 positions were differently cleaved upon low energy collision-induced dissociation. This was reflected in MS/MS analyses by the preferential loss of one of the two fatty acids, leading to a dissymmetrical abundance of the collision fragments, and following dissociation patterns of MS^2 fragments described in previous studies (Abida *et al.*, 2016).

Lipid quantification - The lipid extracts corresponding to about 25 nmol of total fatty acids were dissolved in 100 µL chloroform/methanol [2/1, (v/v)] containing 125 pmol of each internal standard. Internal standards were obtained from Avanti Polar Lipids Inc. for PG 18:0-18:0 or synthesized by D. Lafont (Amara *et al.*, 2009, 2010) for MGDG 18:0-18:0 and DGDG 16:0-16:0 or extracted from spinach thylakoid (Demé *et al.*, 2014) and hydrogenated as previously described for SQDG 16:0-18:0 (Buseman *et al.*, 2006). Lipids were then separated by HPLC and quantified by MS/MS.

The HPLC separation method was adapted from Rainteau *et al.* (2012). Lipid classes were separated using an Agilent 1200 HPLC system using a 150 mm × 3 mm x 5 µm diol column (Macherey-Nagel), at 40°C. The mobile phases consisted of hexane/isopropanol/water/ammonium acetate 1M, pH5.3 [625/350/24/1, (v/v/v/v)] (A) and isopropanol/water/ammonium acetate 1M, pH5.3 [850/149/1, (v/v/v)] (B). The injection volume was 20 µL. After 5 min, the percentage of B was increased linearly from 0% to 100% in 30 min and kept at 100% for 15 min at a flow rate of 200 µL min^{-1}. The distinct glycerolipid classes eluted successively depending on the polar head group.

Mass spectrometric analysis was done on an Agilent 6460 triple quadrupole mass spectrometer equipped with a jet stream electrospray ion source under following settings: Drying gas heater: 260°C, Drying gas flow 13 L min^{-1}, Sheath gas heater: 300°C, Sheath gas flow: 11 L min^{-1}, Nebulizer pressure: 25 psi, Capillary voltage: ± 5000 V, Nozzle voltage ± 1000. Nitrogen was used as the collision gas. The quadrupoles Q1 and Q3 were operated at widest and unit resolution,

612 respectively. SQDG analysis was carried out in negative ion mode by scanning for precursors of m/z -
613 225 at a CE of -56eV. PG, MGDG and DGDG measurements were performed in positive ion mode by
614 scanning for neutral losses of 189 Da, 179 Da and 341 Da at CEs of 16 eV, 8 eV and 8 eV, respectively.
615 Quantification was done by multiple reaction monitoring (MRM) of all the molecules detected in the
616 TLC-MS experiment with 100 ms dwell time. Mass spectra were processed with the Agilent
617 MassHunter Workstation software for lipid identification and quantification. Lipid amounts were
618 corrected for response differences between internal standards and endogenous lipids.
619
620 *Comparative genomics and detection of lateral gene transfers*
621 Among the 53 *Synechococcus* and *Cyanobium* genomes used for comparative analyses in the
622 present study, which encompass marine and halotolerant strains, 22 complete or high quality genome
623 sequences were retrieved mostly from NCBI and 31 are still unpublished. The latter strains were cloned
624 and purified by three transfers onto agarose plates and their DNA extracted, as previously described
625 (Humily *et al.,* 2013). Whole genomes were sequenced by Genoscope (Evry, France) or the NERC
626 Biomolecular Analysis Facility (NBAF) located at the Centre for Genomic Research (University of
627 Liverpool, UK). The genomic sequences were assembled using the CLC Assembly Cell software (CLC Bio,
628 Aarhus, Denmark) and scaffolded using WiseScaffolder (Farrant *et al.*, 2016). After an automatic
629 structural and functional annotation performed by the Institute of Genome Sciences (Maryland, USA)
630 using the Manatee annotation pipeline (http://manatee.sourceforge.net/igs/index.shtml), individual
631 sequences were grouped into clusters of orthologous genes using OrthoMCL (Li et *al.*, 2003), then
632 uploaded into the custom-designed information system Cyanorak v2 (www.cyanorak.sb-roscoff.fr) for
633 further manual curation. All genes involved in the biosynthesis of fatty acids, membrane lipids and
634 acyl-desaturases, as well as 52 ribosomal protein coding genes, were manually curated and their
635 sequences deposited in Genbank (datasets 1-3). The potential occurrence of each acyl-desaturase gene
636 in genomic islands was analyzed using Alien Hunter (Vernikos and Parkhill, 2006).
637
638 *Phylogenetic analyses*
639 Amino acid sequences of the six major acyl-desaturase proteins and 52 ribosomal proteins that
640 were used to make a refined analysis of the phylogeny of marine *Synechococcus* were aligned using
641 MAFFT v7.164b with FFT-NS-2 parameters (Katoh and Standley, 2014). Individual ribosomal protein
642 alignments were then concatenated in one super-alignment of 7,072 amino acid sites and trimmed to
643 remove ambiguously aligned regions using Geneious® 8.1.5 (Kearse *et al.*, 2012). Maximum likelihood
644 trees were inferred using PHYML v3.0 – 20120412 (Guindon and Gascuel, 2003), with the LG
645 substitution model for acyl-desaturase proteins and JTT for the ribosomal proteins, and with the
646 estimation of the distribution of the gamma distribution shape parameter and of the proportion of

invariables sites for both trees. Confidence of branch points was determined by performing bootstrap analyses including 1000 replicate datasets. Phylogenetic trees were edited using the Archaeopteryx v0.9901 beta program (Han and Zmasek, 2009). The single acyl-desaturase tree was drawn using iTOL (http://itol.embl.de; (Letunic and Bork, 2007) and tree comparison was made using the Dendextend R package (Galili, 2015).

Acknowledgements

This work was funded by the French programs ANR *SAMOSA* (ANR-13-ADAP-0010), EMBRC France (INFRA-2010-2.2.5), the French national program EC2CO-MicrobiEn (METALIC) and the National Environment Research Council grant NE/I00985X/1. Justine Pittera was supported by the French Ministry of Higher Education and Research. Solène Breton was supported by the Région Bretagne and the French Ministry of Higher Education and Research. Juliette Jouhet and Eric Maréchal are supported by ANR Investissement d'Avenir Oceanomics and Glyco@Alps. We are grateful to the Roscoff Culture Collection for maintaining the *Synechococcus* strain used in this study. We thank Théophile Grébert for helping during the thermal shift experiments, and Gregory K. Farrant and the ABIMS Platform (Station Biologique de Roscoff) for their help in the genome sequence computing and annotation.

References

Abida H, Dolch L J, Meï C, Villanova V, Conte M, Block MA *et al.* (2015). Membrane glycerolipid remodeling triggered by nitrogen and phosphorus starvation in *Phaeodactylum tricornutum*. *Plant Physiol* 167(1):118-36.

Amara S, Lafont D, Fiorentino B, Boullanger P, Carriere F and De Caro A. (2009). Continuous measurement of galactolipid hydrolysis by pancreatic lipolytic enzymes using the pH-stat technique and a medium chain monogalactosyl diglyceride as substrate. *Biochim Biophys Acta* 1791: 983-990.

Amara S, Barouh N, Lecomte J, Lafont D, Robert S, Villeneuve P *et al.* (2010). Lipolysis of natural long chain and synthetic medium chain galactolipids by pancreatic lipase-related protein 2. *Biochim Biophys Acta* 1801: 508-516.

Awai K, Ohta H, Sato N. (2014). Oxygenic photosynthesis without galactolipids. *Proc Natl Acad Sci USA* 111(37): 13571-13575.

Awai K. (2016). Thylakoid development and galactolipid synthesis in cyanobacteria. In Lipids in Plant and Algae Development, vol. 86 of the series Subcellular Biochemistry pp. 85-101.

Behhrouzian B and Buist PH. (2003). Mechanism of fatty acid desaturation: a bioorganic perspective. *Prostaglandins Leukot Essent Fatty Acid* 68: 107-112.

680 Biller SJ, Schubotz F, Roggensack SE, Thompson AW, Summons RE, Chisholm SW. (2014). Bacterial
681 vesicles in marine ecosystems. Science 343(6167):183-6. doi: 10.1126/science.1243457.
682 Bligh EG and Dyer WJ. (1959). A rapid method for total lipid extraction and purification. *Can J Biochem*
683 *Physiol* 37:911-917.
684 Bogos B, Ughy B, Domonkos I, Laczkó-Dobos H, Komenda J, Abasova L *et al.* (2010).
685 Phosphatidylglycerol depletion affects photosystem II activity in *Synechococcus* sp. PCC 7942 cells.
686 *Photosynth Res* 103(1):19-30.
687 Buseman CM, Tamura P, Sparks AA, Baughman EJ, Maatta S, Zhao J *et al.* (2006). Wounding stimulates
688 the accumulation of glycerolipids containing oxophytodienoic acid and dinor-oxophytodienoic acid
689 in Arabidopsis leaves. *Plant Physiol* 142(1):28-39.
690 Campbell D, Hurry V, Clarke AK, Gustafsson P, Oquist G. (1998). Chlorophyll fluorescence analysis of
691 cyanobacterial photosynthesis and acclimation. *Microbiol Mol Biol Rev* 62: 667-683.
692 Chi X, Yang Q, Zhao F, Qin S, Yang Y, Shen J *et al.* (2008). Comparative analysis of fatty acid desaturases
693 in cyanobacterial genomes. *Comparative and Functional Genomics* 284508.
694 http://doi.org/10.1155/2008/284508.
695 Chintalapati S, Prakash JS, Gupta P, Ohtani S, Suzuki I, Sakamoto T *et al.* (2006). A novel Delta9 acyl-
696 lipid desaturase, DesC2, from cyanobacteria acts on fatty acids esterified to the sn-2 position of
697 glycerolipids. *Biochem J* 398(2):207-14.
698 Chintalapati S, Prakash J SS, Singh AK, Ohtani S, Suzuki I, Murata N *et al.* (2007). Desaturase genes in a
699 psychrotolerant *Nostoc* sp. are constitutively expressed at low temperature. *Biochem Biophys Res*
700 *Comm* 362:81-87.
701 Choi DH and Noh JH (2009). Phylogenetic diversity of *Synechococcus* strains isolated from the East
702 China Sea and the East Sea. *FEMS Microbiol Eco*l 69(3):439-448.
703 Cross B (2016). The Role of PlsX in Fatty Acid Synthesis and Acid Adaptation in *Streptococcus mutans*.
704 Thesis (Ph.D.), University of Rochester. School of Medicine & Dentistry. Dept. of Microbiology &
705 Immunology. 156 pages. http://hdl.handle.net/1802/3097.
706 Demé B, Cataye C, Block MA, Maréchal E and Jouhet J. (2014). Contribution of galactoglycerolipids to
707 the 3-dimensional architecture of thylakoids. *FASEB J.* 28(8):3373-83.
708 Dormann P and Holzl G. (2009). The role of glycolipids in photosynthesis. H. Wada and N. Murata eds.,
709 Lipids in Photosynthesis: Essential and Regulatory Functions, pp. 265-282. Springer Science.
710 Edwards KF, Thomas MK, Klausmeier CA and Litchman E. (2016). Phytoplankton growth and the
711 interaction of light and temperature: A synthesis at the species and community level. *Limnol*
712 *Oceanogr* 61:1232–1244.

713 Farrant G, Doré D, Cornejo-Castillo F, Partensky F, Ratin M, Ostrowski M *et al.* (2016). Delineating
714 ecologically significant taxonomic units from global patterns of marine picocyanobacteria. *Proc Nat*
715 *Acad Sci USA* 113(24): E3365-74. doi: 10.1073/pnas.1524865113.
716 Flombaum P, Gallegos J, Gordillo R, Rincón J, Zabala L, Jiao N *et al.* (2013). Present and future global
717 distributions of the marine cyanobacteria *Prochlorococcus* and *Synechococcus*. *Proc Natl Acad Sci*
718 *USA* 110: 9824-9829.
719 Fork D C, Murata N, Sato N (1979). Effect of growth temperature on the lipid and fatty acid
720 composition, and the dependence on temperature of light-induced redox reactions of cytochrome
721 *f* and of light energy redistribution in the thermophilic blue-green alga *Synechococcus lividus*. *Plant*
722 *Physiol.* 63 (3), 524–530.
723 Galili T (2015). Dendextend: an R package for visualizing, adjusting and comparing trees of hierarchical
724 clustering. *Bioinformatics* 31:3718-3720. doi:10.1093/bioinformatics/btv428.
725 Garwin JL, Klages AL, Cronan JE. (1980). Structural, enzymatic, and genetic studies of beta-ketoacyl-
726 acyl carrier protein synthases I and II of *Escherichia coli*. *J Biol Chem* 255(24):11949-11956.
727 Guindon S and Gascuel O. (2003). A simple, fast, and accurate algorithm to estimate large phylogenies
728 by maximum likelihood. *Syst Biol* 52:696-704.
729 Han MV and Zmasek CM. (2009). phyloXML: XML for evolutionary biology and comparative genomics.
730 *BMC Bioinformatics* 10. doi:Artn 356.
731 Heath R J, Jackowski S and Rock CO. (1994). Guanosine tetraphosphate inhibition of fatty acid and
732 phospholipid synthesis in *Escherichia coli* is relieved by overexpression of glycerol -3-phosphate
733 acyltransferase (*plsB*). *J Biol Chem* 269:26584–26590.
734 Heath R J and Rock C O (1995). Enoyl-acyl carrier protein reductase (*fabI*) plays a determinant role in
735 completing cycles of fatty acid elongation in *Escherichia coli*. *J Biol Chem* 270:26538–26542.
736 Heath RJ, White SW and Rock CO. (2002). Inhibitors of fatty acid synthesis as antimicrobial
737 chemotherapeutics. *Appl Microbiol Biotechnol* 58(6):695-703
738 Herdman M., Castenholz, RW, Waterbury JB and Rippka R. (2015). *Form- Synechococcus*. Bergey's
739 Manual of Systematics of Archaea and Bacteria. 1–7.
740 Hu P, Borglin S, Kamennaya NA, Chen L, Park H, Mahoney L *et al.* (2013). Metabolic phenotyping of the
741 cyanobacterium *Synechocystis* 6803 engineered for production of alkanes and free fatty acids. *Appl*
742 *Energ* 102: 850-859.
743 Huang S, Wilhelm S, Harvey H, Taylor K, Jiao N and Chen F (2012). Novel lineages of *Prochlorococcus*
744 and *Synechococcus* in the global oceans. *ISME J* 6: 285-297.
745 Humily F, Partensky F, Six C, Farrant G K, Ratin M, Marie D *et al.* (2013). A gene island with two possible
746 configurations is involved in chromatic acclimation in marine *Synechococcus*. *PLoS One*
747 8(12):e84459.

748 Iskandar A, Taha BHM, Ahmed RZ, Motoigi T, Watanabe K, Kurasawa N. (2013). Lipids in Cold-adapted
749 Microorganisms. In Cold-Adapted Microorganisms, eds. Isao Yumoto, Caister Academic press,
750 chapter 11, pp. 189-214.
751 Itoh S, Kozuki T, Nishida K, Fukushima Y, Yamakawa H, Domonkos I *et al.* (2012). Two functional sites
752 of phosphatidylglycerol for regulation of reaction of plastoquinone Q(B) in photosystem II. *Biochim*
753 *Biophys Acta* 1817(2):287-97.
754 Johnson Z, Zinser E, Coe A, McNulty N, Woodward E and Chisholm S (2006). Niche partitioning among
755 *Prochlorococcus* ecotypes along ocean-scale environmental gradients. *Science* 311: 1737-1740.
756 Kana P M, Gilbert R, Goericke NA and Welshmeyer TM. (1988). Zeaxanthin and b-carotene in
757 *Synechococcus* WH7803 respond differently to irradiance. *Limnol Oceanogr*, 33:1623–1627.
758 Katoh K and Standley DM. (2014). MAFFT: iterative refinement and additional methods. *Methods Mol*
759 *Biol* 1079:131-146.
760 Kearse M, Moir R, Wilson A, Stones-Havas S, Cheung M, Sturrock S *et al.* (2012). Geneious Basic: an
761 integrated and extendable desktop software platform for the organization and analysis of sequence
762 data. *Bioinformatics* 28(12):1647-1649.
763 Kirchhoff H. (2008). Diffusion of molecules and macromolecules in thylakoid membranes. *Biochim*
764 *Biophys Acta* 1837:495-502.
765 Letunic I and Bork P. (2007). Interactive Tree Of Life (iTOL): an online tool for phylogenetic tree display
766 and annotation. *Bioinformatics* 23:127-128. doi:10.1093/bioinformatics/btl529.
767 Li L, Stoeckert CJ and Roos DS. (2003) OrthoMCL: Identification of ortholog groups for eukaryotic
768 genomes. *Genome Res* 13:2178 -2189.
769 Liu XY, Sheng J and Curtiss R. (2011). Fatty acid production in genetically modified cyanobacteria. *Proc*
770 *Nat Acad Sci USA* 108: 6899-6904.
771 Los DA and Mironov KS. (2015). Modes of fatty acid desaturation in cyanobacteria: An Update. *Life*
772 5(1): 554-567 doi: 10.3390/life5010554.
773 Los D A and Murata N. (2004). Membrane fluidity and its roles in the perception of environmental
774 signals. *Biochim Biophys Acta* 1666:142-157.
775 Los D A and Murata N. (1998). Structure and expression of fatty acid desaturases. *Biochim Biophys Acta*
776 1394:3-15.
777 Ludwig M and Bryant D A (2012). *Synechococcus* sp. strain PCC 7002 transcriptome: acclimation to
778 temperature, salinity, oxidative stress, and mixotrophic growth conditions. *Frontiers in Microbiology*
779 3:354.
780 Mackey K, Paytan A, Caldeira K, Grossman A, Moran D, McIlvin M *et al.* (2013). Effect of temperature
781 on photosynthesis and growth in marine *Synechococcus* spp. *Plant Physiol* 163: 815-829.

782 Marie D, Brussaard C, Partensky F and Vaulot D. (1999). Flow cytometric analysis of phytoplankton,
783 bacteria and viruses. In: Sons JW (ed). *Current Protocols in Cytometry*. International Society for
784 Analytical Cytology. pp 11.11.11-11.11.15.
785 Marsh, D (2010). Structural and thermodynamic determinants of chain-melting transition
786 temperatures for phospholipid and glycolipids membranes. *Biochim Biophys Acta - Biomembranes*
787 1798(1):40–51.
788 Mazard S, Ostrowski M, Partensky F and Scanlan DJ. (2012). Multi-locus sequence analysis, taxonomic
789 resolution and biogeography of marine *Synechococcus*. *Environ Microbiol* 14: 372-386.
790 Meritt M, Rosenstein S P, Rachel C L and Allen M M (1991). A comparison of the major lipid classes and
791 fatty acid composition of marine unicellular cyanobacteria with freshwater species. *Arch Microbiol*
792 155(2):107-113.
793 Moore LR, Goericke R and Chisholm SW. (1995). Comparative physiology of *Synechococcus* and
794 *Prochlorococcus*: influence of light and temperature on growth, pigments, fluorescence and
795 absortive properties. *Mar Ecol Progr Ser* 116:259–275.
796 Mikami K and Murata N. (2003) Membrane fluidity and the perception of environmental signals in
797 cyanobacteria and plants. *Progress in Lipid Research* 42 pp 527-543.
798 Miśkiewicz E, Ivanov AG, Williams JP, Khan MU, Falk S and Huner NP. (2000). Photosynthetic
799 acclimation of the filamentous cyanobacterium, *Plectonema boryanum* UTEX 485, to temperature
800 and light. *Plant Cell Physiol* 41(6):767-75.
801 Mizusawa N, Sakurai I, Sato N and Wada H. (2009a). Lack of digalactosyldiacylglycerol increases the
802 sensitivity of *Synechocystis* sp. PCC 6803 to high light stress. *FEBS Lett* 583(4):718-22.
803 Mizusawa N, Sakurai I, Sato N and Wada H. (2009b). Involvement of digalactosyldiacylglycerol in
804 cellular thermotolerance in *Synechocystis* sp. PCC 6803. *Arch Microbiol* 191(7):595-601.
805 Mizusawa N and Wada H. (2012). The role of lipids in photosystem II. *Biochim Biophys Acta*
806 1817(1):194-208 doi: 10.1016/j.bbabio.2011.04.008.
807 Murata N, Wada H and Gombos Z. (1992). Modes of fatty acid desaturation in cyanobacteria. *Plant Cell*
808 *Physiol* 33:933-941.
809 Murata N and Wada H. (1995). Acyl-lipid desaturases and their importance in the tolerance and
810 acclimatization to cold of cyanobacteria. *Biochem J* 308: 1-8.
811 Nakamura Y, Tsuchiya M and Ohta H. (2007). Plastidic phosphatidic acid phosphatases identified in a
812 distinct subfamily of lipid phosphate phosphatases with prokaryotic origin. *J Biol Chem*
813 2828(1):29013–29021.
814 Ogawa T., Misumi M., Sonoike K. (2017). Estimation of photosynthesis in cyanobacteria by pulse-
815 amplitude modulation chlorophyll fluorescence: problems and solutions. Photosynth Res
816 doi:10.1007/s11120-017-0367-x.

Okazaki K, Sato N, Tsuji N, Tsuzuki M and Nishida I. (2006). The significance of C16 fatty acids in the *sn*-2 positions of glycerolipids in the photosynthetic growth of *Synechocystis* sp. PCC 6803. *Plant Physiol* 141(2), 546–556.

Paulsen M.L., Doré H., Garczarek L., Seuthe L., Müller O., Sandaa RA. *et al.* (2016). *Synechococcus in* the Atlantic Gateway to the Arctic Ocean. *Front. Mar. Sci* doi.org/10.3389/fmars.2016.00191.

Petroutsos D, Amiar S, Abida H, Dolch L J, Bastien O, Rébeillé F *et al.* (2014). Evolution of galactoglycerolipid biosynthetic pathways--from cyanobacteria to primary plastids and from primary to secondary plastids. *Prog Lipid Res* 54:68-85. doi: 10.1016/j.plipres.2014.02.001.

Pittera J, Humily F, Thorel M, Grulois D, Garczarek L and Six C. (2014). Connecting thermal physiology and latitudinal niche partitioning in marine *Synechococcus*. *ISME J* 8: 1221-1236.

Pittera J, Partensky F and Six C. (2016). Adaptive thermostability of light-harvesting complexes in marine picocyanobacteria. *ISME J* doi: 10.1038/ismej.2016.102.

Rainteau D, Humbert L, Delage E, Vergnolle C, Cantrel C, Maubert MA *et al.* (2012). Acyl chains of phospholipase D transphosphatidylation products in *Arabidopsis* cells: a study using multiple reaction monitoring mass spectrometry. *PLoS One* 7(7):e41985.

Rippka R, Coursin T, Hess W, Lichtlé C, Scanlan DJ, Palinska KA *et al.* (2000). *Prochlorococcus marinus* Chisholm et al. 1992 subsp. *pastoris* subsp. nov. strain PCC 9511, the first axenic chlorophyll a_2/b_2-containing cyanobacterium (Oxyphotobacteria). *Intl J Syst Evol Microbiol* 50: 1833-1847.

Rodríguez-Vargas S, Sánchez-García A, Martínez-Rivas J M, Prieto J A and Randez-Gil F (2007). Fluidization of Membrane Lipids Enhances the Tolerance of *Saccharomyces cerevisiae* to Freezing and Salt Stress . Applied and Environmental Microbiology, 73(1), 110–116.

Sakurai I, Hagio M, Gombos Z, Tyystjärvi T, Paakkarinen V, Aro EM *et al.* (2003). Requirement of phosphatidylglycerol for maintenance of photosynthetic machinery. *Plant Physiol* 133(3), 1376–1384.

Sakurai I, Shen J R, Leng J, Ohashi S, Kobayashi M and Wada H. (2006). Lipids in oxygen-evolving photosystem II complexes of cyanobacteria and higher+ plants. *J Biochem (Tokyo)* 140:201-209.

Sakurai I, Mizusawa N, Wada H and Sato N. (2007). Digalactosyldiacylglycerol is required for stabilization of the oxygen-evolving complex in photosystem II. *Plant Physiol* 145(4):1361–1370.

Sanda S, Leustek T, Theisen M, Garavito M and Benning C (2001). Recombinant *Arabidopsis* SQD1 converts UDP-glucose and sulfite to the sulfolipid head group precursor UDP-sulfoquinovose in vitro. *J Biol Chem* 276: 3941–3946.

Sato N and Wada H (2009). Lipid Biosynthesis and its Regulation in Cyanobacteria. H. Wada and N. Murata *eds*., Lipids in Photosynthesis: Essential and Regulatory Functions, pp. 157-177. Springer Science.

851 Sato N (2015). Is monoglucosyldiacylglycerol a precursor to monogalactosyldiacylglycerol in all
852 cyanobacteria? *Plant Cell Physiol* 56(10):1890-1899.
853 Scanlan DJ, Ostrowski M, Mazard S, Dufresne A, Garczarek L, Hess WR, *et al.* (2009). Ecological
854 genomics of marine picocyanobacteria. *Microbiol Mol Biol Rev* 73(2):249-99.
855 Schutt B S, Abbadi A, Loddenkotter B, Brummel M and Spener F (2002). Beta-ketoacyl-acyl carrier
856 protein synthase IV: a key enzyme for regulation of medium-chain fatty acid synthesis in *Cuphea*
857 *lanceolata* seeds. *Planta* 215(5):847-854.
858 Shimojima M, Ohta H and Nakamura Y (2009a). Biosynthesis and Function of Chloroplast Lipids. H.
859 Wada and N. Murata *eds*., Lipids in Photosynthesis: Essential and Regulatory Functions, pp. 35-55.
860 Springer Science.
861 Shimojima M, Tsuchiya M and Ohta H (2009b). Temperature-dependent hyper-activation of
862 monoglucosyldiacylglycerol synthase is post-translationally regulated in *Synechocystis* sp. PCC
863 6803. *FEBS Lett* 2009 583(14):2372-2376.
864 Shivaji S and Prakash JSS. (2010). How do bacteria sense and respond to low temperature? *Arch*
865 *Microbiol* 192(2):85-95.
866 Simionato D, Block M A, La Rocca N, Jouhet J, Maréchal E, Finazzi G *et al.* (2013). The response of
867 *Nannochloropsis gaditana* to nitrogen starvation includes *de novo* biosynthesis of triacylglycerols,
868 a decrease of chloroplast galactolipids, and reorganization of the photosynthetic apparatus.
869 *Eukaryot Cell* 12: 665–676.
870 Six C, Thomas J C, Brahamsha B, Lemoine Y anf Partensky F. (2004). Photophysiology of the marine
871 cyanobacterium *Synechococcus* sp. WH8102, a new model organism. *Aquat Microb Ecol* 35(1), 17–
872 29.
873 Six C, Thomas J, Garczarek L, Ostrowski M, Dufresne A, Blot N *et al.* (2007). Diversity and evolution of
874 phycobilisomes in marine *Synechococcus* spp. – a comparative genomics study. Genome Biol 8:
875 R259.
876 Sohm J, Ahlgren N, Thomson Z, Williams C, Moffett J W, Saito MA *et al.* (2015). Co-occurring
877 *Synechococcus* ecotypes occupy four major oceanic regimes defined by temperature,
878 macronutrients and iron. *ISME J* 10: 333-345 doi: 10.1038/ismej.2015.115.
879 Somerville C, Browse J, Jaworski J G and Ohlrogge JB. (2000). Lipids. In Biochemistry and Molecular
880 Biology of Plants, B. Buchanan, W. Gruissem, and R. Jones, eds (Rockville, MD: American Society of
881 Plant Physiologists), pp. 456–527.
882 Van Mooy BAS, Rocap G, Fredricks HF, Evans CT and Devol AH. (2006). Sulfolipids dramatically decrease
883 phosphorus demand by picocyanobacteria in oligotrophic marine environments. *Proc Nat Acad Sci*
884 *USA* 103 (23):8607-8612 doi: 10.1073/pnas.0600540103

885 Van Mooy BAS, Fredricks HF, Pedler BE, Dyhrman ST, Karl DM, Koblízek M *et al.* (2009). Phytoplankton
886 in the ocean use non-phosphorus lipids in response to phosphorus scarcity. *Nature* 458:69-72.
887 Varkey D, Mazard S, Ostrowski M, Tetu SG, Haynes P and Paulsen IT. (2016). Effects of low temperature
888 on tropical and temperate isolates of marine *Synechococcus*. *ISME J* 10(5):1252-63.
889 Vernikos G S and Parkhill J (2006). Interpolated variable order motifs for identification of horizontally
890 acquired DNA: revisiting the *Salmonella* pathogenicity islands. *Bioinformatics* 22: 2196-203.
891 Wada H and Mizusawa N (2009). The role of phosphatidylglycerol in photosynthesis. H. Wada and N.
892 Murata *eds*., Lipids in Photosynthesis: Essential and Regulatory Functions, pp. 243-263. Springer
893 Science.
894 White S W, Zheng J, Zhang Y M and Rock (2005). The structural biology of type II fatty acid biosynthesis.
895 *Annu Rev Biochem* 74:791–831.
896 Yamamoto Y, 2016. Quality Control of Photosystem II: The mechanisms for avoidance and tolerance of
897 light and heat stresses are closely linked to membrane fluidity of the thylakoids. *Front Plant Sci*
898 7:1136.
899 Zinser E, Johnson Z, Coe A, Karaca E, Veneziano D and Chisholm S (2007). Influence of light and
900 temperature on *Prochlorococcus* ecotype distributions in the Atlantic Ocean. *Limnol Oceanogr* 52:
901 2205-2220.
902 Zwirglmaier K, Jardillier L, Ostrowski M, Mazard S, Garczarek L, Vaulot D *et al.* (2008). Global
903 phylogeography of marine *Synechococcus* and *Prochlorococcus* reveals a distinct partitioning of
904 lineages among oceanic biomes. *Environ Microbiol* 10: 147-161.
905

906 ## Table and figure legends

907 **Table 1:** Genome screening for putative lipid desaturase genes in 53 marine *Synechococcus* and
908 *Cyanobium* genomes, ordered by sub-clusters and phylogenetic clades. Cells filled with grey indicate
909 the presence of one gene copy in the genome. Absence of color indicates that no orthologous gene
910 was found in the genome.

911 **Figure 1:** Variations of growth rate (A), photosystem II quantum yield (F_V/F_M; B), phycobiliprotein
912 fluorescence emission ratio (C) and membrane pigments (D) in *Synechococcus* sp. WH7803 acclimated
913 from 16°C to 30°C. **PE**: Phycoerythrin; **PC**: Phycocyanin; **TA**: Terminal acceptor of the phycobilisome;
914 **Zea**: Zeaxanthin; **β-car**: β-carotene. The measurements were repeated four times.

915 **Figure 2:** Variations in the acyl chains esterified at the two glycerol positions of the four membrane
916 glycerolipids, monogalactosyldiacylglycerol (MGDG), digalactosyldiacylglycerol (DGDG),
917 sulfoquinovosyldiacylglycerol (SQDG) and phosphatidylglycerol (PG) of *Synechococcus* sp. WH7803

acclimated to a range of temperatures (see also Table S2). The left bar chart refers to the fatty acid species bound to the *sn*-1 position, the right one to the fatty acid species bound *sn*-2 position and the *sn*-3 position binds the polar head.

Figure 3: Variations of the acyl chains esterified at the two glycerol positions *sn*-1 (left panels) and *sn*-2 (right panel) of monogalactosyldiacylglycerol (MGDG; A-C), digalactosyldiacylglycerol (DGDG; D-F), sulfoquinovosyldiacylglycerol (SQDG; G-I) and phosphatidylglycerol (PG; J-L), as induced in response to a shift from 22°C to either 13°C (circles) or 18°C (triangles) in *Synechococcus* sp. WH7803. The results are expressed in percentages of total acyl chain esterified at the stereospecific position of the glycerolipid. The experiments were repeated three times.

Figure 4: Variations of the acyl chains esterified at the two glycerol positions *sn*-1 (left panels) and *sn*-2 (right panel) of monogalactosyldiacylglycerol (MGDG; A-C), digalactosyldiacylglycerol (DGDG; D-F), sulfoquinovosyldiacylglycerol (SQDG; G-I) and phosphatidylglycerol (PG; J-L), as induced in response to a shift from 22°C to 30°C, in *Synechococcus* sp. WH7803. The results are expressed in percentages of total acyl chain esterified at the stereospecific position of the glycerolipid. The experiments were repeated three times.

Figure 5: Maximum likelihood analysis of cyanobacterial lipid desaturase enzymes, including marine *Synechococcus, Cyanobium* and a selection of freshwater cyanobacteria (see Supplementary datasets 1-2). Clusters including marine cyanobacteria are shown in green and blue colors while those including exclusively freshwater cyanobacteria are in grey. Circles at nodes indicate bootstrap support over 70%. The scale bar represents the number of substitutions per amino acid position.

Figure 6: Clade- or strain-specific variability of the genomic context for *desc3*, *desC4* and *desA2* genes among the 53 sequenced *Synechococcus* strains. Note that *desA3* is not shown as its genomic context is too variable between strains even within clades. Gene names are indicated as a four letter code except for conserved hypothetical protein genes indicated as “chp” followed by a number. The table shows the acyl-desaturase genes predicted to be located in horizontally transferred genomic islands by the Alien Hunter software, among the 53 *Synechococcus*/*Cyanobium* genomes (http://www.sanger.ac.uk/science/tools/alien-hunter; Vernikos and Parkhill, 2006).

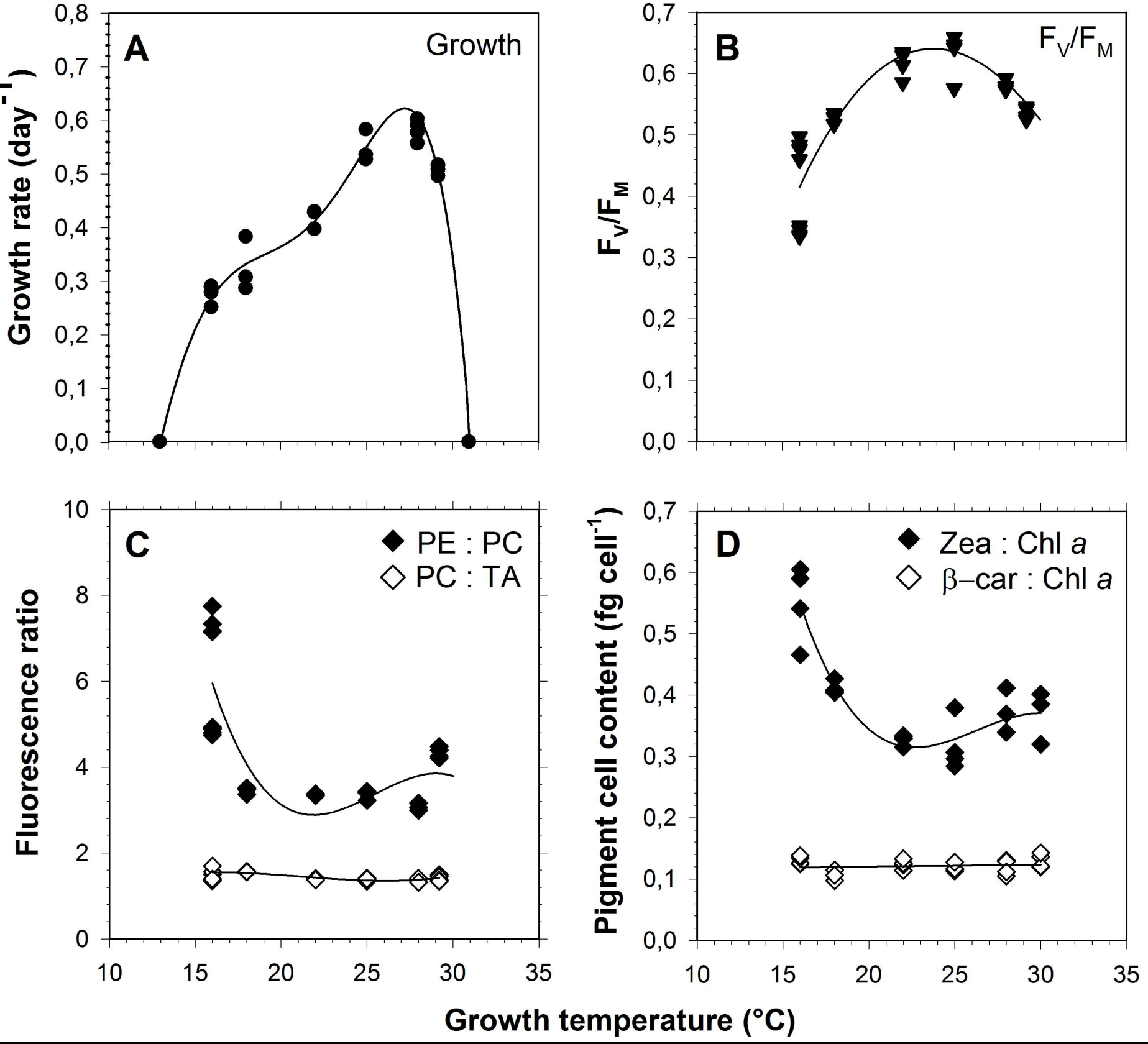
A
Growth
Growth rate (day-1)
0,0
0,1
0,2
0,3
0,4
0,5
0,6
0,7
0,8
B
FV/FM
FV/FM
0,0
0,1
0,2
0,3
0,4
0,5
0,6
0,7
C
PE : PC
PC : TA
Fluorescence ratio
0
2
4
6
8
10
D
Zea : Chl a
β–car : Chl a
Pigment cell content (fg cell-1)
0,0
0,1
0,2
0,3
0,4
0,5
0,6
0,7
10
15
20
25
30
35
Growth temperature (°C)

Pittera *et al.*, Figure 2

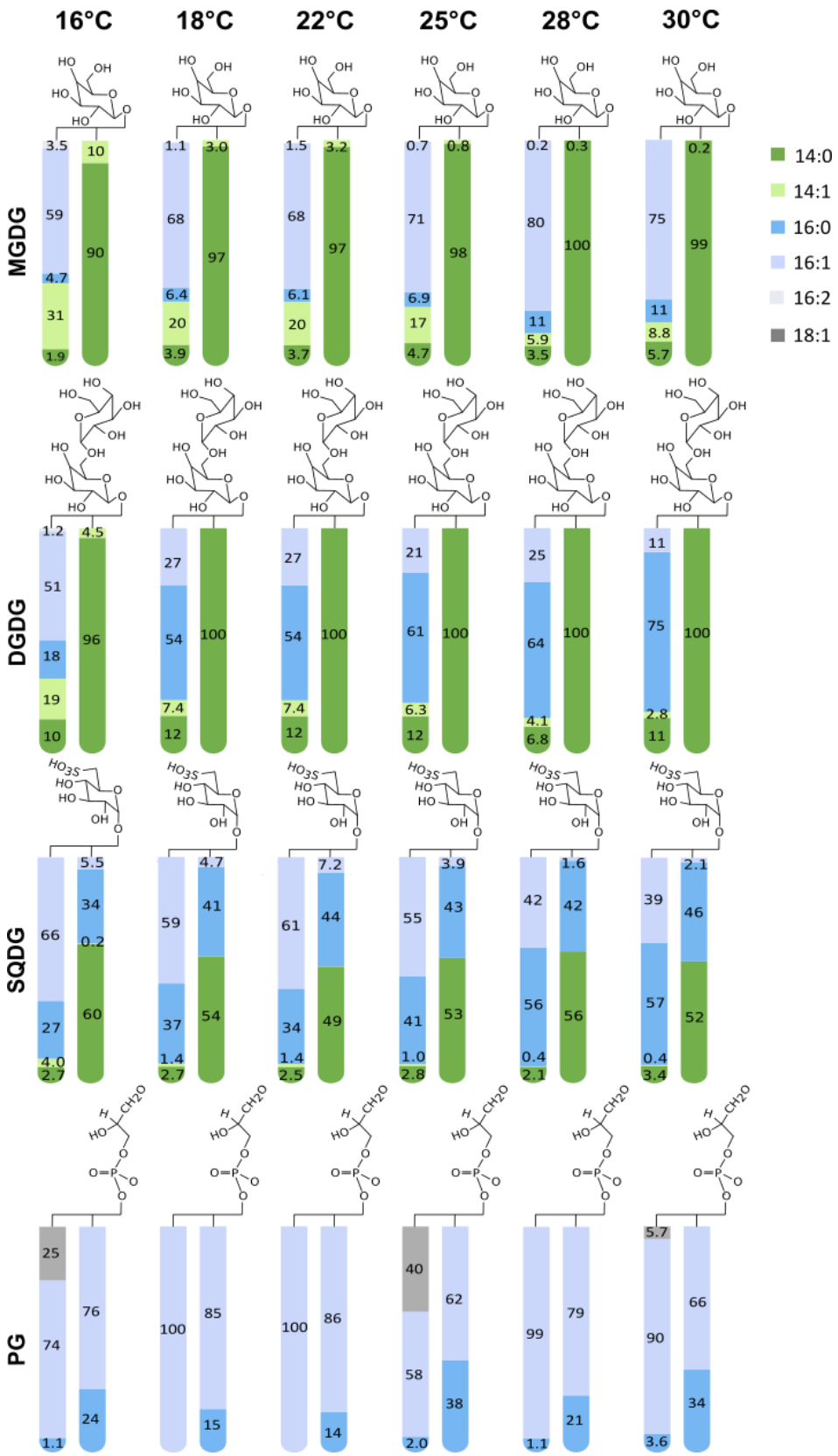

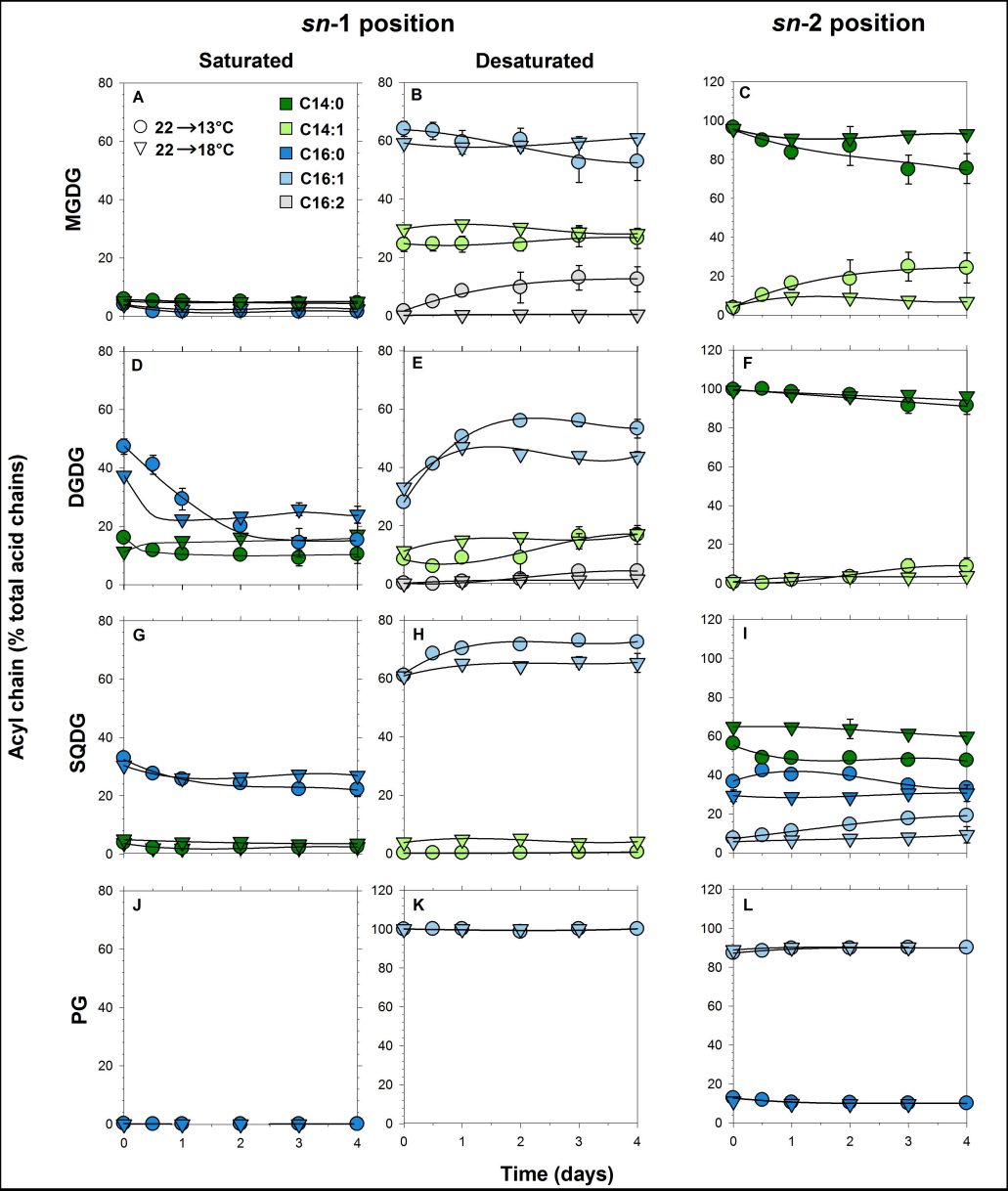
sn-1 position
sn-2 position
Saturated
Desaturated
A
B
C
D
E
F
G
H
I
J
K
L
22 →13°C
22 →18°C
C14:0
C14:1
C16:0
C16:1
C16:2
MGDG
DGDG
SQDG
PG
Acyl chain (% total acid chains)
Time (days)

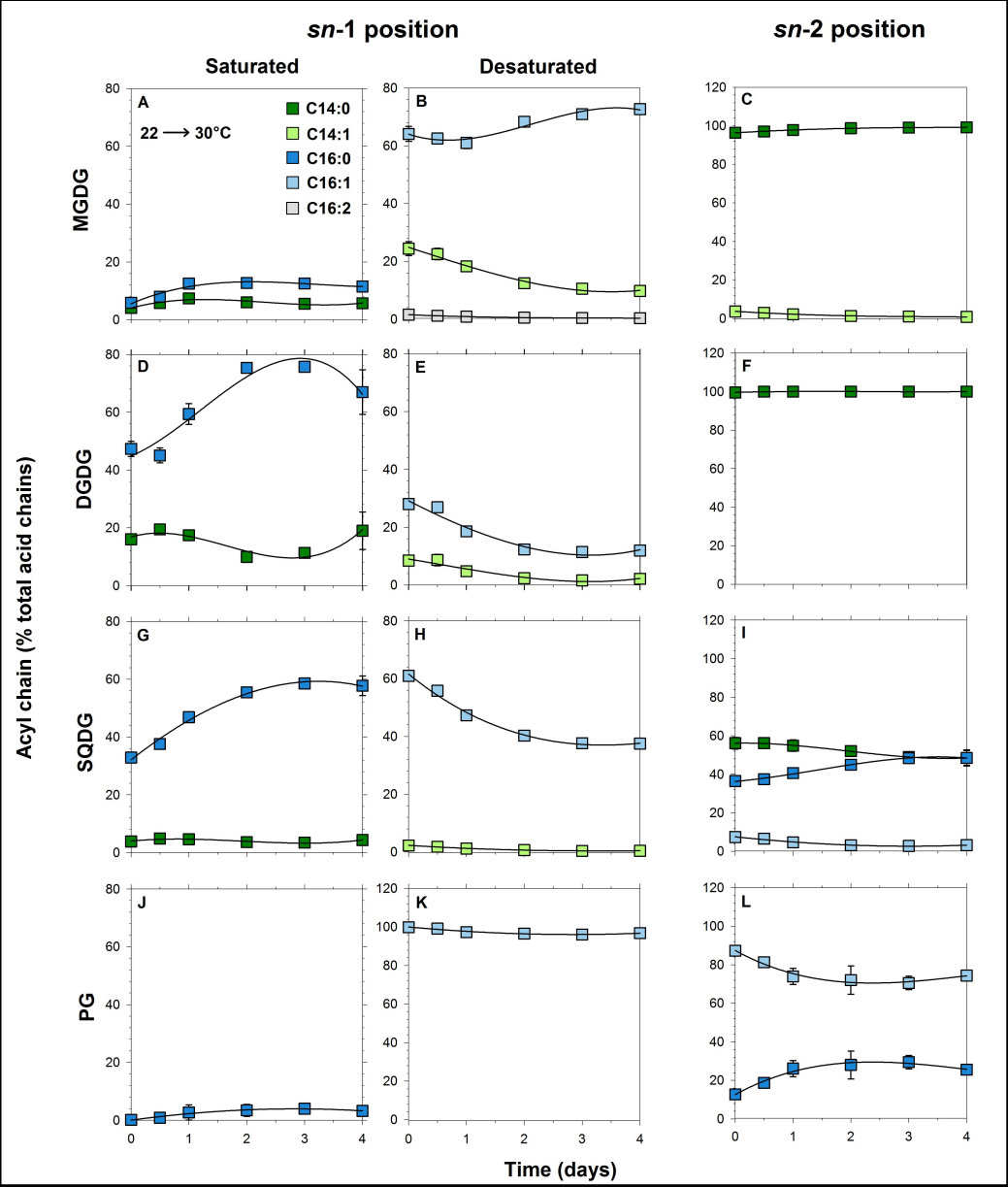
sn-1 position
sn-2 position
Saturated
Desaturated
A
B
C
D
E
F
G
H
I
J
K
L
22 ⟶ 30°C
C14:0
C14:1
C16:0
C16:1
C16:2
MGDG
DGDG
SQDG
PG
Acyl chain (% total acid chains)
Time (days)

Pittera *et al.*, Figure 5

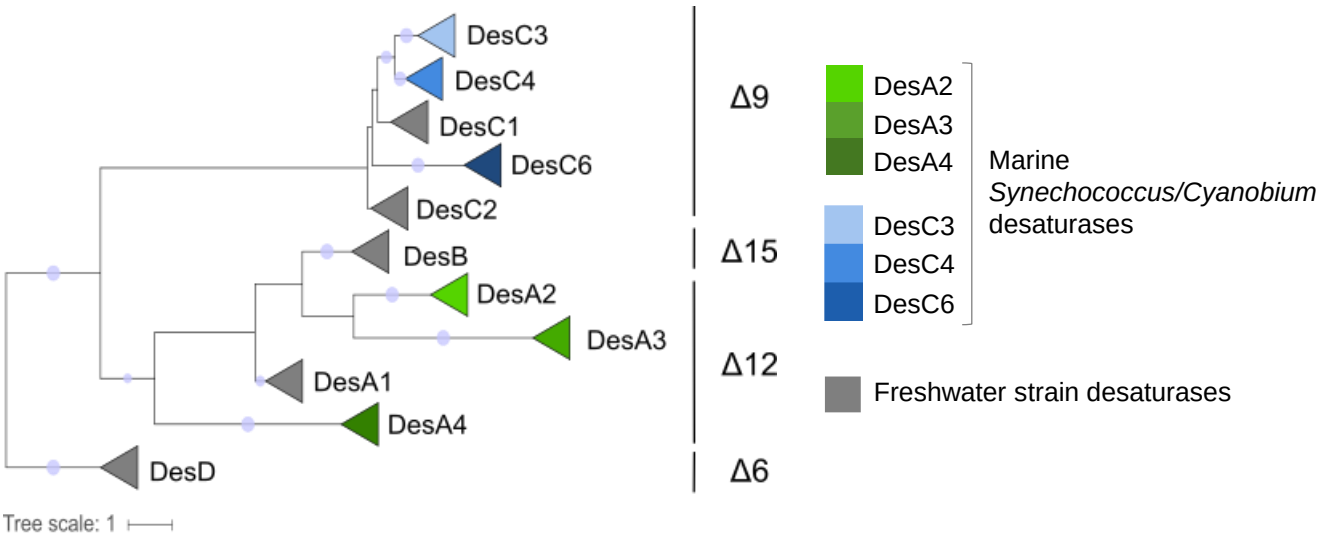

Pittera *et al.*, Figure 6

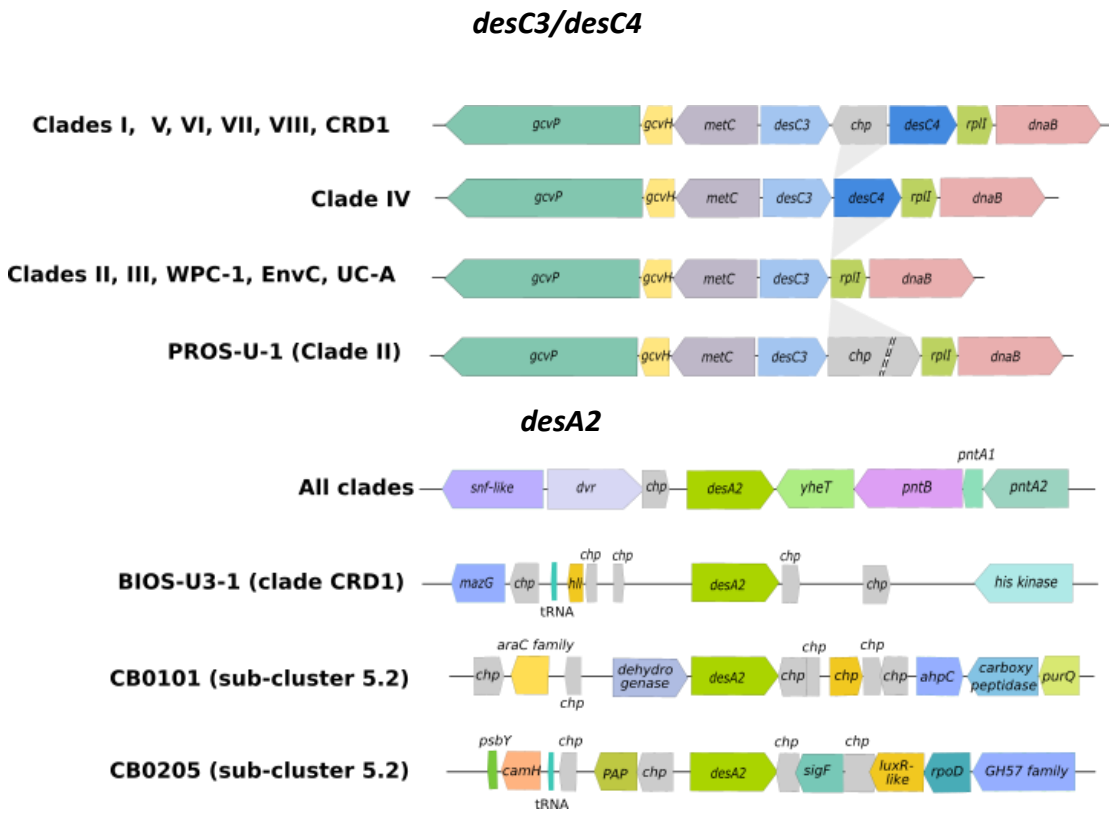

des gene	Prediction for gene inclusion in a genomic island
desC3	No strain
desC4	No strain
desA2	BIOS-U3-1
desA3	A15-24, A15-28, A15-60, A18-25, A18-46, BIOS-E4-1, BIOS-U3-1, BMK-MC-1, CC9616, PROS-U-1, WH8102, WH8109

Table 1

Sub-cluster[1]	Clade[2]	Representative sequenced strains	Δ9 desaturases			Δ12 desaturases			Other desaturases					Number of *des* genes
			desC3	*desC4*	*desC6*	*desA2*	*desA3*	*desA4*	*desC*	*desC*	*des*	*des*	*des*	
5.1	I	CC9311, MVIR-18-1, PROS-9-1, WH8016, ROS8604	■	■			■							3
		SYN20	■	■			■					■		4
	II	A15-62, CC9605, M16.1, RS9902, RS9907, TAK9802	■			■								2
		KORDI-52	■											1
		A15-44	■			■				■				3
		WH8109, PROS-U-1	■			■	■							3
	III	WH8102, WH8103, A15-24, A18-46.1, BOUM118, RS9915, A15-28, A18-40	■			■	■							3
	IV	BL107, CC9902	■	■			■							3
	V	WH7803, BMK-MC-1	■	■		■	■							4
	VI	WH7805, MEDNS5	■	■		■	■							4
		PROS-7-1	■	■		■	■		■		■			6
	VII	A15-60, A18-25c	■	■			■							3
		NOUM97013	■	■		■	■							4
	VIII	RS9909, RS9917	■	■			■							3
		WH8101	■	■										2
	IX	RS9916	■	■										2
	CRD1	MITS9220, BIOS-E4-1	■	■			■							3
		BIOS-U3-1	■	■		■	■							4
	WPC1	A15-127, KORDI-49	■			■	■							3
	XX	CC9616	■				■							2
	UC-A	KORDI-100	■											1
5.2		NS01, WH5701	■	■	■		■	■				■		6
		PCC6307	■	■	■		■	■					■	7
		CB0101	■	■		■	■	■		■				6
		CB0205	■	■		■	■	■						5
		PCC7001	■	■	■			■						4
5.3		RCC307, MINOS11	■	■			■							3

[1] *sensu* Herdman et al. (2001); [2] see Mazard et al. (2012) and Choi & Noh (2009).